

RESEARCH PAPER

**Microneedle assisted permeation of lidocaine carboxymethylcellulose  
with gelatine co-polymer hydrogel**

**Atul Nayak, Diganta B. Das<sup>\*</sup>, Goran T. Vladisavljević**

Department of Chemical Engineering, Loughborough University, Loughborough, LE11 3TU, UK

Accepted for Publication in

**Pharmaceutical Research**

13 September 2013

---

(\*Corresponding author; email: [d.b.das@lboro.ac.uk](mailto:d.b.das@lboro.ac.uk))

1 RESEARCH PAPER

2

3 **Microneedle assisted permeation of lidocaine carboxymethylcellulose with**  
4 **gelatine co-polymer hydrogel**

5

6 **Atul Nayak, Diganta B. Das<sup>\*</sup>, Goran T. Vladisavljević**

7

8 Department of Chemical Engineering, Loughborough University, Loughborough, LE11 3TU, UK.

9

10 (\*Corresponding author; email: [d.b.das@lboro.ac.uk](mailto:d.b.das@lboro.ac.uk))

11

12 **ABSTRACT**

13

14 **Purpose** Lidocaine hydrochloride (LidH) was formulated in sodium carboxymethyl cellulose/  
15 gelatine (NaCMC/GEL) hydrogel and a 'poke and patch' microneedle delivery method was used  
16 to enhance permeation flux of LidH.

17

18 **Methods** The microparticles were formed by electrostatic interactions between NaCMC and GEL  
19 macromolecules within a water/oil emulsion in paraffin oil and the covalent crosslinking was by  
20 glutaraldehyde. The GEL to NaCMC mass ratio was varied between 1.6 and 2.7. The LidH  
21 encapsulation yield was 1.2 to 7% w/w. LidH NaCMC/GEL was assessed for encapsulation  
22 efficiency, zeta potential, mean particle size and morphology. Subsequent in vitro skin  
23 permeation studies were performed via passive diffusion and microneedle assisted permeation  
24 of LidH NaCMC/GEL to determine the maximum permeation rate through full thickness skin.

25

26 **Results** LidH 2.4% w/w NaCMC/GEL 1:1.6 and 1:2.3 respectively, possessed optimum zeta  
27 potential. LidH 2.4% w/w NaCMC/GEL 1:2.3 and 1:2.7 demonstrate higher pseudoplastic  
28 behaviour. Encapsulation efficiency (14.9-17.2%) was similar for LidH 2.4% w/w NaCMC/GEL  
29 1:1.6-1:2.3. Microneedle assisted permeation flux was optimum for LidH 2.4% w/w NaCMC/GEL  
30 1:2.3 at 6.1 µg/ml/h.

31

32 **Conclusion** LidH 2.4% w/w LidH NaCMC/GEL 1:2.3 crossed the minimum therapeutic drug  
33 threshold with microneedle skin permeation in less than 70 min.

34

35 **Keywords** lidocaine, sodium carboxymethylcellulose, gelatine, hydrogel, microneedles, in vitro  
36 skin permeation

## 37 INTRODUCTION

38 The delivery of local anaesthesia to lacerated skin regions remains a major challenge for  
39 injectable and ointment drugs (1). For example, the subcutaneous injection delivery of local  
40 anaesthetics, specifically lidocaine hydrochloride (LidH), is clinically reported to cause a burning  
41 type feeling when infused directly into the skin. Also, LidH requires additional active drug  
42 molecules in an ointment formulation to compete with injectable LidH (1-3). A bolus dosage of  
43 LidH by injection is suitable for short duration of action (1-4). However, the treatment of multiple  
44 lacerations in skin may need co-drugs such as epineprine to aid longer time for LidH action,  
45 which may be ineffective due to a shorter sustained subcutaneous infiltration or simply a second  
46 bolus injection after the first lag time (4-6). Lidocaine's characteristic amide functional group (7)  
47 and its weak base molecule (pKa 7.7) with a lipophilic function while permeating through  
48 biological membranes is still a highly attributable choice of local anaesthesia since its first  
49 chemical synthesis in 1943 (7,8). Similarly, the protonated LidH is a weakly acidic, hydrophilic  
50 molecule which is easily soluble in water at ambient temperature. Injectable LidH solution in  
51 either the basic or acidic form shares the same local anaesthetic mechanism for the antagonism  
52 of nerve signals in cells by inhibiting the influx of sodium ions through the sodium channels of  
53 biological cell membranes resulting in a response to temporary pain blockage on the skin surface  
54 (9-11). LidH is dependent on a drug vehicle as a support material with respect to viscoelastic  
55 bulking and balancing of the encapsulation efficiency with enhanced skin permeation  
56 pharmacokinetics. Sodium carboxymethylcellulose (NaCMC) polymer and gelatine (GEL) co-  
57 polymer, according to a defined mass ratio are suitable candidates in mapping the crosslinking  
58 structure with the functional role of trapping LidH and with the goal for optimised skin permeation  
59 pharmacokinetics (12).

60  
61 Fig. 1a  
62

63 Sodium carboxymethylcellulose and gelatine (NaCMC/GEL) microparticulates form covalent  
64 linkages between NaCMC's hydroxyl group lactonisation with the aldehyde of glutaraldehyde's -  
65 CHO group in the formation of ether bonds under low pH conditions (12) (Fig. 1a). A schiff base  
66 association between glutaraldehyde and gelatine is formed by covalent linkage in minimising  
67 ionic dissociation between NaCMC with GEL in neutral media (12,13) (Fig 1a). Also, ionic  
68 interactions occur between polyanionic NaCMC, glycine and proline amino acids of a  
69 polycationic GEL and cationic LidH with the effect of charge neutralisation (14,15) (Fig 1b).  
70 Overall, this process forms a pH sensitive hydrogel network of NaCMC intertwined with GEL  
71 crosslinks for trapping active molecules such as LidH (16,17). The most ideal pH for  
72 electrostatically crosslinking NaCMC with GEL is at pH 4.0 from the view point of zeta potential  
73 analysis. The LidH NaCMC/GEL vehicles are hydrogel microparticles because of pH sensitivity  
74 across a factor of 3.5 which interrupts the electrostatic interactions, allowing the release of  
75 trapped drug molecules (18). In the context of electro-ionic interactions concerning the  
76 formulation, there is no significant quantitative study on ionic interactions between NaCMC, GEL  
77 and LidH with respect to potentiometric measurements, pH thresholds and polarography analysis.  
78 These are fairly important parameters for relating ionic properties but zeta potential analysis  
79 looks into the dispersion of microparticles in the hydrogel as a result of the degree in like charge

80 repulsion which is discussed later. The microparticles in LidH NaCMC/GEL hydrogel alone  
81 cannot optimise skin permeation kinetics and a minimally invasive skin puncturing device is  
82 essential in aiding the optimisation of skin permeation kinetics. Recent advances in microneedle  
83 technology promises to resolve this issue and allow microneedle assisted LidH delivery from  
84 NaCMC/GEL hydrogel.

85 Fig. 1b  
86

87 Microneedles are minimally invasive micron scale needles protruding perpendicularly from a  
88 laterally mounted platform. It is a painless method of micro-injection for not hitting pain receptors  
89 concentrated in the dermal layer of skin (19). The planar surface and geometrical properties of  
90 the microneedles, and the texture of skin, which is relatively impermeable to large aqueous,  
91 active molecules and drug molecules in a bulk polymeric formulation, can increase permeation  
92 through the viable epidermal layer of skin via micro channel cavities created by microneedles  
93 (20,21). Biomedical grade stainless steel is a suitable metallic alloy for microneedles as it allows  
94 for fast and economical shape cutting to specific dimensions in-conjunction to retaining its highly  
95 desirable compressive strength properties (21,22). For example, we find that Type 304 stainless  
96 steel has been chosen to prepare microneedles in some studies because of its biocompatibility  
97 and inherently good compressive and shear force properties (23).

98  
99 Recent advances in lidocaine delivery methods involved liquid crystalline polymeric microneedle  
100 arrays which successfully delivered 71% of LidH by mass using a coat and poke method with a  
101 therapeutic level maintained for approximately five minutes (24). Solid microneedles were also  
102 structured from solution components of lidocaine, mixed with sodium chondroitin sulfate and  
103 cellulose acetate as water soluble vehicles (25). Skin permeation analysis sustained a  
104 therapeutic threshold of lidocaine between 89-131  $\mu\text{g/g}$  for an approximate duration of two and a  
105 half minutes before crossing the maximum therapeutic level pertaining toxicity greater than  
106 131 $\mu\text{g/g}$  for over ten minutes (25). A detailed review explaining the current material properties,  
107 fabrication process and pharmacokinetic delivery of LidH in polymeric microneedles are  
108 discussed in detail by Nayak and Das (26).

109  
110 The development of LidH NaCMC/GEL hydrogel coupled with microneedle delivery via a poke  
111 and patch method is a promising approach (26). The approach requires no additional active co-  
112 drugs when formulated with NaCMC/GEL polymeric mass ratios as the most abundant drug  
113 vehicle reagents. Co-drugs for LidH significantly add to the cost of the final product than NaCMC  
114 and GEL vehicles in abundance. However, at the moment, there is little known about the  
115 significance of microneedle assisted permeation of LidH from the micro-particles in NaCMC/GEL  
116 hydrogel, and in particular, the relationship of the permeation kinetics with the geometrical  
117 parameters of microneedles, e.g., the length of the microneedles. In addressing these issues,  
118 this work aims to develop a LidH formulation in NaCMC/GEL hydrogel and, explore, for the first  
119 time, a poke and patch microneedle delivery method for the purpose of improved drug  
120 permeation rates and permeation flux of LidH. The overall goal is towards an optimised  
121 cumulative amount of lidocaine in watery plasma media, enhanced lidocaine permeation flux and  
122 encapsulation efficiency in-conjunction with a sustained therapeutic permeation range  
123 transdermally of over fifteen minutes. As explained in detail previously, LidH, as a weak acid, can  
Page 4 of 22

124 be bound electrostatically within soluble drug vehicles consisting of crosslinked NaCMC and GEL  
125 macromolecules. NaCMC, GEL and glutaraldehyde are cheap, biocompatible and readily  
126 available compounds as potential drug formulas in constructing a carrier for LidH. LidH  
127 molecules diffuse from the electrostatically formed microparticle to the surrounding deionised (DI)  
128 water, analogous to the watery plasma of the viable epidermis of skin. The operation of the poke  
129 and patch technique allows for LidH from hydrogel to permeate through microneedles formed  
130 holes on the skin and dissolve into the viable epidermis. The microparticles in the LidH  
131 NaCMC/GEL hydrogel are hydrophilic in nature. A concentration gradient between LidH  
132 NaCMC/GEL hydrogel and underlying watery plasma of skin allows for LidH to dissociate from  
133 NaCMC/GEL hydrogel and associate as lidocaine into the neutral watery plasma. Skin  
134 permeating rates will be compared for passive diffusion and microneedle assisted diffusion of  
135 LidH NaCMC/GEL hydrogels.

136

## 137 **MATERIALS AND METHODS**

138 A laboratory scale batch process for the formulation of LidH NaCMC/GEL hydrogel is highly  
139 advantageous with respect to low heat treatment and quite efficient preparation times in reaching  
140 the desired product. The high degree of carboxylate substitution of NaCMC of 0.9 enhances the  
141 possibility of greater crosslinking with type A, i.e., high bloom gelatine. As explained in the  
142 introduction, the crosslinking is electrostatically achievable at pH 4. LidH is a favourable drug  
143 molecule in association with NaCMC/GEL at pH 4 for encapsulation purposes. The  
144 glutaraldehyde is necessary in defining spherical microparticles from water in oil (w/o) droplets.

145

### 146 **Materials**

147 Sodium carboxymethylcellulose (degree of substitution (DS): 0.9; molecular weight (MW): 250  
148 kD), sorbitan monooleate (SPAN 80), glutaraldehyde (stock solution of 50% w/w), paraffin liquid  
149 (density: 0.859 g/ml), LidH (MW: 288.81 g/mol) and porcine gelatine (type A, Bloom 300) were  
150 purchased from Sigma-Aldrich Ltd, Dorset, UK. Acetic acid (analytical grade), acetonitrile (HPLC  
151 grade), ammonium bicarbonate (analytical grade) and n-hexane (95% w/w) were purchased from  
152 Fisher Scientific Ltd, Loughborough, UK. Deionised (DI) water was the common solvent for  
153 aqueous solutions unless otherwise stated.

154

### 155 **Constant encapsulation of drug LidH in hydrogel of different NaCMC/GEL mass ratios**

156 The mass ratio of NaCMC/GEL outlines one of the formulation characteristics in relation to LidH  
157 pharmacokinetics in this study. Therefore, different NaCMC/GEL mass ratio polymers were  
158 encapsulated with a constant LidH dosage. The individual reagents/chemicals chosen for this  
159 purpose are represented in Table i. A non-ionic surfactant, Span 80 (0.5% w/w), was dispersed  
160 dropwise in 100 ml of light paraffin oil, which was stirred at 400 rpm in a rotating vessel (IKA-  
161 Werke, Staufen, Germany) until a homogeneous mixture was formed. Aqueous NaCMC (1.2%  
162 w/w) was then dispersed dropwise into the paraffin/surfactant mixture with shear induced at 400  
163 rpm using the same rotating vessel followed by aqueous dropwise dispersion of gel ( $C_{GEL}$ , % w/w)  
164 until a viscous w/o emulsion was formed (Table i). The variable mass percentage of the GEL is  
165 denoted by the term  $C_{GEL}$ .

166

167

Table i
---------

168

169 In the next step, the pH of the w/o mixture was decreased to pH 4 using acetic acid (~ 1% w/w).  
170 LidH (2.4% w/w) was then dispersed drop wise into the emulsion and cooled in a refrigerator (4-  
171 6°C) for 30 minutes. The cooled LidH NaCMC/GEL emulsion was agitated in a rotating vessel  
172 (IKA-Werke, Staufen, Germany) at 400 rpm to re-suspend the emerging hydrogel microparticles  
173 before the drop wise addition of glutaraldehyde (0.1% w/w). The w/o droplets were transformed  
174 into microparticles by the glutaraldehyde and stirred at 1000 rpm for a duration of 2 hours to  
175 ensure thorough mixing. The resultant LidH NaCMC/GEL formulation was stored at 2-4°C in a  
176 laboratory refrigerator (Liebherr-Great Britain Ltd, Biggleswade, UK) for a period of 4 h to allow  
177 for the separation of residual paraffin liquid (organic layer) from a dense LidH NaCMC/GEL  
178 formulation layer. The organic layer was cloudy in appearance as compared with the lower  
179 dense layer. After refrigeration, the organic layer was syringe removed. The refrigerated LidH  
180 was mixed with an organic solvent, n-hexane (50% v/v) for the subsequent removal of residual  
181 organic solvent. Any remaining residual organic solvent was oven dried under vacuum at 40°C to  
182 enhance solvent evaporation (Technico, Fistreem International Ltd, Loughborough, UK). Finally,  
183 any unbound LidH was removed through filter washing with DI water. The grade 3 filter  
184 (Whatman International Ltd, Oxon, UK) that was used for the formulation washing stage had an  
185 average pore size of 6 µm. The LidH NaCMC/GEL hydrogels were collected in amber vials and  
186 characterised for passive diffusion and microneedle assisted skin permeation.

187

#### 188 **Different encapsulation of drug LidH in hydrogel of constant NaCMC/GEL mass ratio**

189 The plausible effect of varying LidH concentration on constant NaCMC/GEL mass ratios is  
190 necessary in exploring significant changes in pseudoplasticity and microparticle dispersion. In  
191 this case, the preparation methods and conditions were replicated as those adopted for constant  
192 LidH encapsulation experiments described earlier. However, on this occasion, the initial LidH  
193 concentration in the NaCMC/GEL hydrogel was varied in the range 1.2-7.0% w/w prior to  
194 achieving a hydrogel of certain NaCMC/GEL mass ratio. LidH NaCMC/GEL with 1:1.6 and 1:2.3  
195 mass ratios of microparticles were prepared to evaluate visco-elasticity and zeta potential effects  
196 for a variable LidH encapsulated concentration (Table i).

197

#### 198 **The Unloaded NaCMC/GEL 1:2.3 mass ratio hydrogel**

199 The effect of pH on zeta potential for unloaded NaCMC/GEL 1:2.3 mass ratio hydrogel was used  
200 as a control in this study to explore the ideal pH conditions for microparticle dispersion.  
201 Unencapsulated GEL to NaCMC mass ratio of 2.3 for hydrogel microparticles, which were  
202 devoid of LidH, were replicated from the same methods and conditions as for the constant LidH  
203 encapsulation to evaluate the zeta potential effects (Table i).

204

#### 205 **In vitro permeation of LidH from NaCMC/GEL microparticles**

206 A Franz diffusion cell for vitro skin permeation was used in exploring and understanding the  
207 pharmacokinetics of LidH prepared with different NaCMC/GEL mass ratios. The Franz diffusion  
208 cell is a common method for transdermal permeation studies. It has two compartments which  
209 comprises of a donor (open cylinder lid) and a receptor. The skin sample is sandwiched between  
210 the two compartments (27). The donor compartment represents the interface between the drug  
211 component and skin surface (28). In particular, this research infers the receptor compartment is

212 the interface between lower viable epidermis/upper dermis regions of porcine skin with deeper  
213 dermis layer of skin in the water plasma, receptor compartment (28). In this work, microneedle  
214 assisted diffusion of LidH NaCMC/GEL (Fig. 2) were studied using full thickness porcine skin. All  
215 skin samples were excised from an ear auricle with approximate dimensions of 20.0 x 20.0 x  
216 0.73 mm which were acquired from four to five months old piglets and stored at -20.0°C. The  
217 procurement of swine auricles were confirmed to be pre-washed in plain water and purchased in  
218 a non-mutilated condition from swine cadaver. An approximate force of 0.57N per array  
219 perpendicular to the base was directed on AdminPatch microneedles (Nanobiosciences,  
220 Sunnyvale, CA, USA) pre-fabricated from stainless steel with arrow head geometry. The  
221 microneedles were applied on the skin for a total duration of 5 minutes. This corresponds to the  
222 time duration we needed to pierce the skin without bending or damaging the microneedle. We  
223 wanted to ensure that each experiment with microneedle is conducted for a consistent time of  
224 application and thumb force. From our experiments (e.g, staining experiments) we found that it  
225 was necessary to apply the microneedles for about 5 minutes on the skin sample before we  
226 obtained detectable holes on the MN. Many microneedles (e.g., those which are coated with  
227 drugs or biodegradable in nature) are designed to stay in the skin for longer duration (e.g., 30 – 4  
228 hours) so that the drugs loaded on the microneedles are released. This is not the case in this  
229 study and we apply the microneedles for 5 minutes to create the holes on the skin. The force  
230 inducer supporting a flat based punch dye was lowered below the flat microneedle base before  
231 the application of forces was directed on the microneedle array by hand leverage. At the end of 5  
232 minutes the applied force was released, the microneedle array was carefully removed and a  
233 constant mass of LidH formulation ( $0.10 \pm 0.03\text{g}$ ) was placed on the skin. This technique is a two  
234 stage process commonly described as “poke and patch” (29) where the “patch” in this context is  
235 the applied hydrogel formulation.

Fig. 2

239 It is known that the penetration depth of the microneedles is less than the actual microneedle  
240 lengths. Further, the penetration depth depends on the microneedle density on the patch,  
241 providing all other factors (e.g., tissue) remaining the same. From the histology of the skin with  
242 and without microneedles, we observe that the lengths of the holes created by the microneedle  
243 are roughly about 50-60% of the actual microneedle length for normal thumb force applied in this  
244 work.

246 Passive diffusion studies (Fig. 2) using LidH NaCMC/GEL hydrogel were conducted on the  
247 adjacent section of the same square skin section of precisely the same average dimensions as  
248 previously stated. The same mass of formulation ( $0.10 \pm 0.03\text{g}$ ) was placed onto the middle of  
249 the skin to conduct the passive diffusion studies. The Franz diffusion cell set up with a receptor  
250 compartment aperture area of  $1.93 \pm 0.0005 \text{ cm}^2$  was connected to an instrument module in  
251 supporting water circulation and magnetic stirring induction used in measuring the permeation  
252 kinetics of LidH through the skin. The stratum corneum layer in skin was facing the donor lid and  
253 the dermis layer was facing the receptor aperture. The skin surface which is part of the stratum  
254 corneum layer was exposed to a room temperature of 20°C. A stretchable parafilm seal (Fisher  
255 Scientific, Loughborough, UK) placed on the open aperture lid of the donor compartment

256 prevented air influx to the receptor compartment during syringe removal of DI water. The  
257 receptor compartment which has a volume of  $5.3 \pm 0.05$  ml contained DI water at  $37.0^\circ\text{C}$  stirred  
258 at 300 rpm to represent a well-mixed liquid. Unlike most clinical studies concerning physiological  
259 pH mimicked by phosphate buffer solution (30), this work used DI water with respect to  
260 mimicking watery plasma in the lower viable epidermis layer of skin. The use of DI water is  
261 consistent with developmental stage of in vitro skin permeation studies (31). A receptor volume  
262 ( $1.5 \pm 0.05$  ml) was syringe removed (Cole-Palmer, Hanwell, UK) at 30 minutes and subsequent  
263 1 hour intervals. This amount was put in a centrifuge vial and centrifuged (1300 rpm) for 6  
264 minutes and the clear supernatant was pipetted out into 2ml vials for HPLC-DA (Agilent  
265 technologies, Wokingham, UK) analysis of LidH concentration. All HPLC analyses were  
266 performed within 24 hours of sample collection from the Franz cell receptor. The results were  
267 obtained in duplicate which were then used to determine average pharmacokinetic variables for  
268 further analysis. The permeation flux was calculated based on two data sets of mass ratio  
269 hydrogel formulations, plotted with error bars representing the random error at 90 % confidence  
270 level.

271  
272 In this work, the in vitro permeation of LidH were interpreted by constructing a profile of  
273 cumulative amount of the drug against time as distinct charts in the section for both microneedle  
274 assisted and passive diffusion. A percentage adjustment of 28.0% was calculated from taking the  
275 1.5ml syringe removal volume as the numerator and the 5.3ml receptor compartment volume as  
276 the denominator in obtaining a percentage from a fraction. This percentage adjustment (28.0%)  
277 from the previous dilution was added to the next detected concentration during a lapsed time  
278 period in obtaining a cumulative concentration profile. The cumulative concentration detected  
279 was interpreted into a more tangible parameter of cumulative amount permeated when taking  
280 into account of the receptor compartment's distinct aperture. The cumulative amount permeated  
281 (Q) was determined by equation (1) (32,33) with coefficient,  $C_x$ , the lidocaine concentration in  
282 receiver compartment at the specific time (h), V - volume of DI water in receptor compartment  
283 (ml) and A - cross sectional diffusion area of receptor aperture ( $\text{cm}^2$ ).

$$285 \quad Q = \frac{C_x V}{A} \quad (1)$$

286  
287 The flux permeation at steady state ( $J_s$ ) was determined by Fick's first law using equation (2) with  
288 coefficients,  $\Delta m/\Delta t$ , the amount of drug permeating through the skin per incremental time at  
289 steady state ( $\mu\text{g}/\text{h}$ ) (34,35).

$$291 \quad J_s = \frac{\Delta m}{A \Delta t} \quad (2)$$

### 292 293 **Analysis of particle size distribution**

294 The particle size distributions in the hydrogel were analysed using laser diffraction particle size  
295 analyser (Series 2000, Malvern Instruments, Malvern, UK). The data were obtained in duplicate  
296 per repeated hydrogel mass ratio sample via superimposition of data points and the particle size  
297 distributions were plotted as particle diameter against percentage particle volume. Particle



298 diameters were compared at 10% ( $d_{10}$ ), 50% ( $d_{50}$ ) and 90% ( $d_{90}$ ) regions of total percentage  
299 particle volume. The refractive index of water as the continuous phase medium was adapted in  
300 determining hydrogel microparticle sizes for the particle size analyser.

301

### 302 **Determination of LidH encapsulation efficiency (EE)**

303 The experimentally determined amount of LidH contained in a sample of NaCMC/GEL  
304 microparticles was interpreted in terms of encapsulation efficiency (EE). For the purpose of  
305 determining LidH encapsulation efficiency, a sample weight (5.0%) of LidH GEL/NaCMC  
306 microparticles was measured. DI water representing excess watery plasma ( $20.0 \text{ ml} \pm 0.1 \text{ ml}$ )  
307 was pipetted into the weighed LidH hydrogel sample and heated to  $37.0 \pm 1^\circ\text{C}$  in a pre-heated  
308 bath (Grant Instruments Ltd, Shepreth, UK). This sample was then sonicated using a commercial  
309 sonifier (Fisher Scientific, Loughborough, UK) at 35W for 10 minutes. It was then filtered using  
310 Nylon 6,6 membranes of  $0.1\mu\text{m}$  pore size (Posidyne membranes, Pall Corporation, Portsmouth,  
311 UK) under gentle vacuum using a Buchner filter setup (Fisher Scientific, Loughborough, UK).  
312 The filtrate was immediately dispensed into a HPLC vial of volume 1.5 ml. The HPLC results  
313 were obtained in triplicate which were then used to determine the mean percentage  
314 encapsulation efficiency by using equation 3 (36,37).

315

$$\% \text{ EE} = \left[ \frac{\text{actual 5.0\% weight of LidH from polymeric ratio sample (g)}}{5.0\% \text{ theoretical encapsulation weight of LidH}} \right] \times 100 \quad (3)$$

316

### 317 **Zeta potential analysis**

318 The measurement of zeta potential provides a valid indication for microparticle dispersion with  
319 respect to charged particle repulsion between microparticles, and as such, the zeta potential of  
320 the microparticles was measured in this study. Ideal zeta potential thresholds will be discussed in  
321 detail later. The zeta potential of LidH-loaded microparticles was measured using a zetasizer  
322 (Malvern 3000 HAS, Malvern, Malvern, UK). The microparticles in the developed LidH  
323 NaCMC/GEL hydrogel ( $2.0 \pm 0.5 \text{ g/ml}$ ) diluted in DI water were injected into the sample port,  
324 temperature maintained at  $20.0^\circ\text{C}$  and the results were obtained in duplicate. Unloaded  
325 NaCMC/GEL 1:2.3 mass ratio hydrogels without any LidH were also subject to zeta potential  
326 analysis. Likewise, the temperature was maintained at  $20.0^\circ\text{C}$  and the results were obtained in  
327 duplicate.

328

### 329 **Measurement of viscosity**

330 The viscoelastic property of the variable LidH NaCMC/GEL hydrogel formulation requires  
331 investigation so as to maintain consistency of the formulation and since the rheological  
332 properties of the hydrogel affects its flow through the holes created by the microneedles. In this  
333 case, we used a rotational viscometer (Haake VT 550, Thermo Fisher Inc, Massachusetts, USA)  
334 for determination of bulk (average) dynamic viscosity of the samples of LidH NaCMC/GEL  
335 hydrogels (maximum volume 25 ml). An NV cup and rotor segment (dimensions of length: 60  
336 mm and radius: 20.1 mm) with a gap of 0.35mm was acquired after a brief qualitative  
337 observation of samples as a thick, semi-solid texture. The shear rate was ramped from  $1 \text{ s}^{-1}$  to  
338  $200 \text{ s}^{-1}$  and held constant at  $200 \text{ s}^{-1}$  for 30 s. The viscosity measurement experiments were  
339 carried out at ambient condition of  $20^\circ\text{C}$ . NaCMC/GEL hydrogel is not a thermoresponsive

340 polymer, so the effects of viscosity against temperature at different, shear rates were not  
341 considered in the paper. Rheological properties of the hydrogel in this paper represent the  
342 normal condition for storage at ambient temperature and not the body temperature.

343

#### 344 **Optical micrography of microparticles in LidH NaCMC/GEL hydrogel**

345 The microparticles in LidH NaCMC/GEL hydrogel are visible optically and the increasing mass of  
346 Gel in the LidH NaCMC/GEL hydrogel provides a significant trend in microparticle morphology. A  
347 sample volume of ~30  $\mu$ l containing the microparticles of LidH NaCMC/GEL hydrogel was  
348 pipetted onto a slide placed on the stage of an optical microscope (BX 43, Olympus, Southend-  
349 on-Sea, UK) which was used to obtain the micrographs.

350

#### 351 **Analysis of LidH concentration using high performance liquid chromatography (HPLC)**

352 LidH concentrations were analysed by using HPLC. The mobile phases in eluting LidH were  
353 acetonitrile (HPLC grade) and 10mM ammonium bicarbonate solution (pH 7.5), respectively, in  
354 an isocratic gradient ratio of 50:50. The flow rate of 0.4 ml/min and column temperature of  
355 20.0°C (Perkin Elmer, Series 1100, Cambridgeshire, UK) was kept constant. LidH molecule was  
356 detected by a diode array detector with the wavelength set at 210 nm (Agilent, Series 1100,  
357 Berkshire, UK). The system's tube lines were purged after eluent degassing with helium. The  
358 baseline corrections were performed before the injection of 5 $\mu$ l of LidH standard and a  
359 characteristic peak was identified and recorded.

360

361 Standard solutions of lidocaine hydrochloride were prepared in ultrapure water with  
362 concentrations ranging from 1.0 to 64.0  $\mu$ g/ml from a stock solution of 1.0 mg/ml. Each standard  
363 solution was analysed by HPLC in duplicate to obtain a linear profile of known concentration  
364 against mean area under curve of the integrated lidocaine peak. The HPLC column  
365 specifications are Gemini-NX 3 $\mu$ m particle size of reverse phase, C18 compound composition  
366 and physical dimensions of 100 x 2 mm, which was purchased from Phenomenex, Cheshire, UK.  
367 The mean area under signal peak corresponding to serial standard concentrations for LidH (0.5-  
368 64.0 ppm) was plotted with a linear regression analysis ( $R^2= 0.999$ ) which showed very good  
369 agreement with the data points.

370

## 371 **RESULTS**

372 Desirable trends and outlines of results are organised with sub-headings concerning LidH  
373 NaCMC/GEL hydrogel formulation and pharmacokinetics of LidH permeation through the skin  
374 with relation to therapeutic levels.

375

#### 376 **Encapsulation of LidH in NaCMC/GEL microparticles**

377 The mean percentage of LidH encapsulated in the NaCMC/GEL microparticles as a function of  
378 mass ratio of NaCMC to GEL is plotted in Fig. 3. LidH 2.4% w/w NaCMC/GEL 1:2.7 mass ratio  
379 showed the highest encapsulation efficiency of 32% (standard deviation (SD) = 1.2%) as  
380 compared with the microparticles of lower NaCMC/GEL polymeric ratios.

381

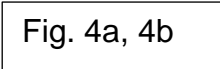
382

383

Fig. 3

### 384 **Viscoelasticity of LidH NaCMC/GEL hydrogel**

385 The results in this work (Fig. 4a) suggest that the increase in LidH concentration had no  
386 significant effect on the average dynamic viscosity of the hydrogel. In particular, the data points  
387 after the shear rate of  $100 \text{ s}^{-1}$  outlined a single asymptote and they superimposed well (Fig. 4a).  
388 The minimum dynamic viscosity of constantly encapsulated LidH NaCMC/GEL hydrogels (Fig.  
389 4b) from the shear range 100 to  $200 \text{ 1/s}$  asymptote is found to be  $0.14 \text{ Pa}\cdot\text{s}$  for LidH  
390 NaCMC/GEL 1:2.0 mass ratio, which may provide a low pseudo plasticity to the hydrogel. Within  
391 the shear range 100 to  $200 \text{ sec}^{-1}$  asymptotes of  $0.28$  and  $0.31 \text{ Pa}\cdot\text{s}$  are found for LidH  
392 NaCMC/GEL 1:2.3 and 1:2.7 mass ratios, respectively and they account for little difference in  
393 pseudo plasticity. But a marked difference in pseudo-plasticity is observed when LidH  
394 NaCMC/GEL 1:2.0 mass ratio is compared with LidH NaCMC/GEL 1:2.7 mass ratio (Fig 4b).  
395 Substantially, there is no significant difference in shear thinning dynamic viscosity induced by a  
396 constant maximum shear of  $200 \text{ s}^{-1}$  when comparing LidH 2.4% w/w NaCMC/GEL variable mass  
397 ratio hydrogels. This outlines very good reproducibility with SD of 0.02 for each LidH  
398 NaCMC/GEL hydrogel mass ratios (Fig. 5).

399  
400  Fig. 4a, 4b

401  Fig. 5

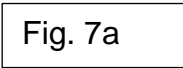
### 402 **Distribution of microparticles in LidH NaCMC/GEL hydrogel**

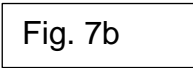
403 The particle size distribution curves were noticeably similar for LidH 2.4% w/w NaCMC/GEL  
404 1:2.3 and 1:2.7 mass ratios with the same mean particle diameter of  $140 \mu\text{m}$  (Fig. 6) for each  
405 one. As found, the  $d_{10}$  values were  $29 \mu\text{m}$  and  $35 \mu\text{m}$  for LidH NaCMC/GEL 1:2.3 and 1:2.7 mass  
406 ratios, respectively. Also, the  $d_{90}$  values were  $305 \mu\text{m}$  and  $277 \mu\text{m}$  for LidH NaCMC/GEL  
407 1:2.3 and 1:2.7 mass ratios, respectively (Fig. 6). The particle size distribution was considerably  
408 left skewed, less broad in describing the peak outline for LidH 2.4% w/w NaCMC/GEL 1:1.6  
409 mass ratio with a mean particle diameter of  $98.65 \mu\text{m}$  where  $d_{10} = 19.3 \mu\text{m}$  and  $d_{90} = 301.78 \mu\text{m}$   
410 were recorded (Fig. 6).

411  Fig. 6

### 414 **Zeta potential of LidH NaCMC/GEL mass ratio and pH effects in microparticles**

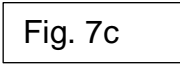
415 In developed microparticles, LidH loading ranges from 1.2-2.8% w/w for NaCMC/GEL 1:1.6 mass  
416 ratio resulted in no significant change in zeta potential (SD = 0.09) and showed excellent  
417 reproducibility in comparison to the high zeta potential values and poor reproducibility of LidH 7.0%  
418 w/w NaCMC/GEL 1:1.6 mass ratio (SD = 1.84) (Fig: 7a). LidH 2.4% wt and 2.8% wt, loaded each  
419 in NaCMC/GEL 1:1.6 and 1:2.3 mass ratios showed good reproducibility (SD = 0.10 and SD =  
420 0.05 respectively) and desirably low zeta potential values approaching  $-40 \text{ mV}$  (Fig. 7b).

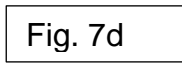
421  
422  Fig. 7a

423  Fig. 7b

424 LidH 2.4% w/w NaCMC/GEL 1:1.6 till 1:2.3 mass ratios provided desirably low zeta potential  
425 values approaching  $-40 \text{ mV}$  and good reproducibility (SD = 0.76) compared with LidH  
426 NaCMC/GEL 1:2.7 mass ratio in which the zeta potential was undesirably high and, hence,  
427 agglomeration was more significant due to the high gelatine concentration (Fig. 7c). The  
Page 11 of 22

428 hydrogel microparticles may have unbound gelatine flocculating and diverting the innermost  
429 negative charge boundaries of defined LidH loaded NaCMC/GEL microparticles. LidH 2.4% and  
430 2.8% w/w encapsulated NaCMC/GEL 1:2.3 mass ratio depict desirable and stable zeta potential  
431 values close to -40 mv despite LidH 2.8% w/w loaded NaCMC/GEL 1:2.3 mass ratio outlining a  
432 slightly lower reproducibility (SD = 0.80) (Fig. 7d). Also LidH 7.0% w/w encapsulated  
433 NaCMC/GEL 1:2.3 mass ratio depicted a repeat of the high zeta potential behaviour in terms of  
434 an undesirably high and slightly more agglomeration effect due to high loading of LidH (Fig. 7d).

435  
436  Fig. 7c

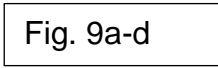
436  Fig. 7d

437  
438 The effect of pH on NaCMC/GEL 1:2.3 resulted in  $f(x) = -2.8x^3 + 50.5x^2 - 273.1x + 404.4$  (Fig. 8)  
439 where  $f(x) = \zeta$  (mV). A good fit from low standard deviation, error bars represented close  
440 agreement between experimentally determined data and theoretical data (Fig. 8).

441  Fig. 8

#### 442 443 **Morphology of microparticles in LidH NaCMC/GEL hydrogel**

444 The micro-particles of LidH 2.4% w/w NaCMC/GEL 1:1.6 to 1:2.7 mass ratio were found to be  
445 spherical. However they show small areas of agglomeration with respect to microparticulate  
446 hydrogel morphology (Fig. 9a.-9d). The microparticles in LidH 2.4% w/w NaCMC/GEL 1:1.6,  
447 1:2.3 and 1:2.7 mass ratios appear slightly more distinct spherically and dispersed with less  
448 agglomeration compared with LidH 2.4% w/w NaCMC/GEL 1:2.0 mass ratio. More significantly in  
449 the quantity with regards to larger microparticle sizes were observed for LidH 2.4% w/w  
450 NaCMC/GEL 1:2.7 mass ratio hydrogel (Fig. 9d).

451  Fig. 9a-d

#### 452 453 454 **Microneedle assisted and passive diffusion of LidH from NaCMC/GEL hydrogel**

455 Clinical research has shown that LidH in plasma fluid is able to sustain localised drug action at a  
456 normal threshold range of 1.2 to 5.5  $\mu\text{g/ml}$  or 3.11  $\mu\text{g/cm}^2$  to 14.25  $\mu\text{g/cm}^2$  after conversion into  
457 cumulative permeated amounts for LidH (47,48). Microneedle assisted diffusion of LidH  
458 NaCMC/GEL 1:2.3 mass ratio showed a fast time taken for the cumulative amount permeated at  
459 1.1 h after crossing the minimum LidH therapeutic level. Comparatively, the same LidH  
460 formulation used for passive diffusion studies showed the fastest time in crossing the minimum  
461 therapeutic level regarding the cumulative amount permeated was 1.5 h (Fig 10a). During the  
462 microneedle assisted diffusion of LidH NaCMC/GEL, 1:1.6 and 1:2.0 mass ratios both outlined  
463 faster times taken for the cumulative amount permeated past 1.25 h when extrapolated towards  
464 a minimum LidH therapeutic level. Comparatively the passive diffusion of LidH NaCMC/GEL  
465 1:1.6 mass ratio and passive diffusion of LidH NaCMC/GEL 1:2.0 mass ratios crossed the  
466 minimum therapeutic level at 2h and 3h, respectively (Fig. 10a). The error bars from duplicate  
467 data sets showed very good reproducibility (Fig 10a). Permeated rates of microneedle assisted  
468 LidH NaCMC/GEL hydrogels recorded in the first 0.5 h, were significantly high for 1:2.3 mass  
469 ratio with a 20.5 fold increase when compared with passive diffusion and low for 1:2.0 mass ratio  
470 with a 1.4 fold increase compared with passive diffusion (Fig. 10b). Likewise as discussed, the  
471 error bars from duplicate data sets showed good reproducibility (Fig 10b).

472  
473  
474  
475  
476  
477  
478  
479  
480  
481  
482  
483  
484  
485  
486  
487  
488  
489  
490  
491  
492  
493  
494  
495  
496  
497  
498  
499  
500  
501  
502  
503  
504  
505  
506  
507  
508  
509  
510  
511  
512  
513  
514  
515

Fig. 10a

Fig. 10b

LidH NaCMC/GEL 1:1.6 mass ratio formulation represented the lowest microneedle assisted permeation flux of  $3.8 \mu\text{g}/\text{cm}^2/\text{h}$  (Fig. 10c) despite a low microparticle size diameter of nearly  $99 \mu\text{m}$  compared with other NaCMC/GEL mass ratio formulations. In theory smaller microparticles should allow greater ease in passing skin pores and diffusing water plasma in the lower regions of the skin. Nevertheless the zeta potential results with respect to a very low zeta correlating to greater dispersion than agglomeration of microparticles is the main supporting concept for high permeation flux. The random error of permeation flux for the duplicate data sets showed good reproducibility (Fig 10c).

Fig. 10c

## DISCUSSION

### Surfactant and oil based continuous phase medium in emulsion stage preparation

Paraffin oil as the continuous phase mixed with non-ionic surfactant, SPAN 80 (sorbitan monooleate), for stabilising aqueous emulsion droplets possessed ideal properties (38). Comparatively SPAN 20, SPAN 40 and SPAN 60 series were unsuitable surfactants because SPAN 80 is the most hydrophobic and accounts for much slower emulsion phase inversion from W/O to W/O/W (38). However, a water content in the range of 10 -15% w/w and temperature at  $60^\circ\text{C}$  allow for emulsion phase inversions in SPAN 20 and SPAN 80 (38). This phase inversion phenomenon is highly unlikely to occur as the temperature of the LidH NaCMC/GEL emulsion was kept below  $35^\circ\text{C}$  despite the aqueous phase content was determined above 15% w/w. Paraffin oil, continuous phase medium aided the dispersion of polar droplets before further addition of glutaraldehyde for microparticle formation. The n-octanol/water partition coefficient of paraffin oil is noted,  $\log P > 3.5$  (Fisher Scientific Ltd, Loughborough, UK) and the non-polarity is attributed to the high interfacial tension and lower dielectric constant in terms of % w/w solubilisation (39). The formation of a NaCMC/GEL polymeric hydrogel network is to entrap and crosslink a linear polymeric structure with a more branched structure in considering covalent bonding interactions to a lesser extent, thus permitting intermolecular dissociation in a continuous phase such as water (40,41). Glutaraldehyde was used for fixing and strengthening the crosslinking of a polymer and co-polymer to form spherically shaped microparticles (42).

### The effect of increasing Gel concentration on encapsulation efficiency of LidH NaCMC/GEL

Gelatine in greater concentrations in hydrogel NaCMC/GEL microparticles influences the gelling properties of the hydrogel matrix with respect to crosslinking with NaCMC at low pH via electrostatic charges and hypothetically creating a more complex intertwined mesh to trap LidH molecules. In order to gain a better insight into the reason for a substantially valid increase in encapsulation efficiency from 1:2.3 mass ratio NaCMC/GEL to 1:2.7 mass ratio requires electro-analytical research with respect to overall ionic charge distribution effects. However this is not within the scope of this current paper.

516 **Visco-elastic and particle diameter properties of LidH NaCMC/GEL hydrogel**

517 LidH is weakly acidic and the positively charged tertiary amide in it has no effect on influencing  
518 the pseudoplasticity of the NaCMC/GEL hydrogel (Fig. 4a). Increasing the GEL ratio  
519 concentration component in the LidH polymeric hydrogel microparticles slightly increases the  
520 pseudoplasticity of the hydrogel formulation caused by gelling thus appearing more pronounced  
521 with respect to LidH NaCMC/GEL 1:2.3 and 1:2.7 mass ratios. This has an influence on creating  
522 bigger microparticle sizes as discussed later in particle size distribution (Fig. 6). Mild  
523 pseudoplasticity is a common viscoelastic property for LidH NaCMC/GEL hydrogels despite low  
524 values pointing to shear thinning at a maximum shear of 200 1/s (Fig. 4a and 5).

525

526 The reduced hydrogel matrix properties caused by a much lower gelatine ratio concentration for  
527 LidH NaCMC/GEL hydrogel despite a constant high shear of 1000 rpm during the formulation  
528 preparation stages has a significantly profound decrease of mean particle size diameter when  
529 comparing NaCMC/GEL 1:1.6 mass ratio with NaCMC/GEL 1:2.3 and 1:2.7 mass ratios (Fig. 6).  
530 Morphologically larger microparticles in LidH NaCMC/GEL hydrogel are distinctly represented for  
531 the 1:2.7 mass ratio with respect to the highest concentration of GEL co-polymer (Fig. 9). A  
532 similar polymeric GEL microparticle study (43) obtained volume mean particle size range from  
533 247-535 $\mu$ m for 1:4 and 1:9 NaCMC/GEL ratio non-steroidal anti-inflammatory drug (NSAID)  
534 mainly because of low overhead stirring speeds of 400 rpm, high viscosity grade NaCMC (500-  
535 800 mPas) and higher co-polymer, gelatine concentration in the ratio mixture.

536

537 **Polyelectrostatic LidH NaCMC/GEL and Unloaded NaCMC/GEL microparticles on zeta**  
538 **potential**

539 A high concentration of weakly acidic LidH in a low polycationic GEL weight ratio NaCMC/GEL  
540 hydrogel formulation is likely to influence slightly more agglomeration of microparticles. Also the  
541 high LidH concentration disrupted the complex coacervate formation before the permanent  
542 fixation and assembly of droplets into defined spherical microparticles by glutaraldehyde (Fig. 7a).  
543 Low agglomeration was already deduced from low zeta potential values and there was no  
544 significant difference for further reduced agglomeration and metastable particle stability when  
545 LidH 2.4% wt or 2.8% w/w is encapsulated in either NaCMC/GEL 1:1.6 or 1:2.3 mass ratios,  
546 respectively (Fig. 7b). However LidH 7.0% w/w loaded in NaCMC/GEL 1:1.6 and 1:2.3 mass  
547 ratios showed significantly higher, positive, zeta potential values and therefore slightly more  
548 agglomeration of microparticles (Fig. 7b).

549

550 The zeta potential effect of charged particles with a charge distribution density on the inner core  
551 provides a good indication of a metastable and non-agglomerated particulate hydrogel in the  
552 empirically determined range of -31.0 to -40.0 mV (44,45). The surface charges in the  
553 microparticles of LidH NaCMC/GEL hydrogel are negative due to dissociation of acidic groups on  
554 GEL and LidH contributing to an acidic environment in forming a spherical core shell structure in  
555 conjunction to electronegative DI water molecules, basic carboxylate groups in NaCMC and  
556 conjugate base of acetic acid contribute to the outermost shell boundary (45,46). Zeta potential is  
557 a fairly common and valid analytical technique for determining the LidH NaCMC/GEL  
558 microparticles in dispersal from weak acid medium of pH 4.0 to a near neutral plasma pH  
559 medium. Placebo NaCMC/GEL hydrogel microparticles outline the minima ( $d\zeta/d(\text{pH}) = 0$ ) which

560 is representative of the lowest zeta value showed the most desirable pH value at -58.6 mV (Fig.  
561 8) so pH 4.0 was the ideal and adapted pH for NaCMC/GEL overall hydrogel media in the  
562 encapsulation of LidH. Above acidic conditions of pH 4.0 for the placebo NaCMC/GEL 1:2.3  
563 mass ratio resulted in a gradual increase in zeta potential which is likely caused by reduction in  
564 dissociated polycationic GEL and polyanionic NaCMC, and microparticle agglomeration is more  
565 defined.

566

### 567 **LidH from NaCMC/GEL hydrogels as a transdermally permeating agent**

568 The minimum therapeutic and toxic level permeation thresholds values were taken from  
569 references (47,48), converted from micrograms per millilitre concentration of LidH into  
570 micrograms per square centimetres for permeated concentration using equation 1 and  
571 expressed using constants derived from Franz diffusion cell receptor compartment volume and  
572 receptor area of aperture in equation (4).

573

$$574 \quad Q = \frac{5c}{1.93} \quad (4)$$

575

576 Commercially acquired AdminPatch microneedles (Nanobiosciences, Sunnyvale, CA, USA)  
577 created channels and widened skin pores for the drug to bypass the stratum corneum layer and  
578 diffuse into the viable epidermis. Staining techniques have shown similar length AdminPatch  
579 microneedles to penetrate beyond the SC layer of skin from a recent study (31). Imperatively the  
580 use of microneedles is to allow the drug to diffuse just above the minimum therapeutic levels at  
581 lower recorded time durations than passive diffusion which is devoid of any needles.

582

583 The effective diffusional area in considering the barrier diffusing membrane properties of skin  
584 was adapted from Fick's first law for explaining the permissible trends for passive diffusion and  
585 microneedle assisted cumulative diffusion of LidH NaCMC/GEL hydrogels through the skin. The  
586 LidH 2.4% w/w NaCMC/GEL hydrogels are permeating the uppermost layer, highly lipophilic  
587 layer of skin very slowly for upto 30 minutes (Fig. 10b). After thirty minutes, the permeating  
588 amount of LidH diffuses at a much faster rate because the lower section layer of skin is less  
589 lipophilic and pseudo steady state conditions are observed for all LidH NaCMC/GEL hydrogels  
590 after 1.5 hours (Fig 10a). LidH NaCMC/GEL microparticles enter the opened microneedle treated  
591 skin cavity while for passive diffusion the hair follicles and sweat pores are the natural cavities for  
592 these microparticles (49). The natural cavities in skin are considerably smaller openings when  
593 compared with post microneedle ones (49). Excised skin used in vitro will generally have lower  
594 moisture content because of high trans-epidermal water loss (TEWL) values and microparticles  
595 will tend to cause a reservoir effect in viable or dermis layers of skin (50). After thirty minutes, the  
596 permeating amount of LidH diffuses at a much faster rate because the lower section layer of skin  
597 is less lipophilic and pseudo steady state conditions are observed for all LidH NaCMC/GEL  
598 hydrogels after 1.5 hours (Fig 10a).

599

600 The cumulative skin permeation of the three LidH 2.4% w/w NaCMC/GEL hydrogels depicted  
601 good overall high rates than compared with passive diffusion, especially past the time of 0.5 h  
602 (Fig 10a and 10b). Emerging plateau levels of cumulative permeation amounts through skin

603 were already documented post 4.5 h. However, the aim for a higher LidH amount permeated  
604 past minimum therapeutic levels were particularly targeted at the most plausible shorter time  
605 duration than a long sustained release profile hence comparative cumulative permeation studies  
606 were conducted in a short time range.

607

608 Increasing the gel concentration in a LidH 2.4% w/w NaCMC/GEL hydrogel outlined an increase  
609 in permeation flux for both passive diffusion and microneedle assisted permeation (Fig. 10c).  
610 LidH 2.4% w/w NaCMC/GEL mass ratio 1:2.3 showed a highly favourable permeation flux with  
611 respect to microneedle assisted delivery of LidH. The encapsulation efficiency of LidH 2.4% w/w  
612 NaCMC/GEL mass ratios are similar and therefore cannot explain the effect of increasing LidH  
613 release rates when the Gel mass ratio is increased in the hydrogel vehicle in terms of correlating  
614 with an unchanged encapsulation efficiency just above 15%. However, LidH 2.4% w/w  
615 NaCMC/GEL mass ratio 1:2.7 provided a substantially high encapsulation efficiency of 32% and  
616 a reciprocally poor, highly insignificant, low value skin permeation flux which was interpreted as a  
617 no result. A high gelatine mass weight of 3.3% w/w in LidH 2.4% w/w NaCMC/GEL mass ratio  
618 1:2.7 hydrogel provided for a more compacted gelling and adsorbing properties, thus preventing  
619 the release of a detectable quantity of LidH. The high gelation of LidH 2.4% w/w NaCMC/GEL  
620 mass ratio 1:2.7 microparticles are responsible for agglomeration by high zeta potential (Fig. 7c).  
621 However, LidH 2.4% w/w NaCMC/GEL mass ratio 1:2.3 had a slightly higher and a favourably  
622 closer zeta potential to -40 mV and therefore the permeation flux for passive diffusion and  
623 microneedle assistance is influenced to be highest because of less microparticulate  
624 agglomeration or clustering effect.

625

## 626 **CONCLUSION**

627 LidH NaCMC/GEL is a highly potential and promising hydrogel formulation requiring microneedle  
628 assisted delivery to excel low passive diffusion flux rates by relatively significant proportions.  
629 Microneedle assisted LidH 2.4% w/w NaCMC/GEL mass ratio 1:2.3 hydrogel is found to be the  
630 most ideal formulation for exceeding the minimum therapeutic permeation threshold of  
631  $3.11\mu\text{g}/\text{cm}^2$  just after 70 minutes but requiring removal before 140 minutes. A seventy minute  
632 duration for pseudo steady state permeation, concerning LidH 2.4% w/w NaCMC/GEL mass ratio  
633 1:2.3 is highly beneficial in numbing the immediate skin region in a hypothetical case of multiple  
634 lacerations in close proximity that require wound cleaning and suturing.

635

636 LidH 2.4% w/w is the most ideal loading concentration for NaCMC/GEL 1:1.6 and 1:2.3 mass  
637 ratio hydrogel because of reproducible and stable approaching values of -40.0 mV zeta potential.  
638 A buffered pH 4.0 was essential in the induction of an anionic polymer and cationic co-polymer  
639 polyelectrolyte interaction and facilitation of dispersed hydrogel microparticles as measured by a  
640 zeta of -58 mV. There are significant differences in visco-elasticity caused by polymeric ratios of  
641 NaCMC and Gel than the constant loading concentration of LidH when an ideal polymeric mass  
642 ratio 1:2.3 is implemented.

643

644 The envisaged aim for LidH NaCMC/GEL as an ideal painless, local anaesthetic formulation  
645 remains in the early developmental stage due to further challenges in reduction of residual  
646 paraffin oil content, scope for smaller micron scale particle sizes and subsequently higher



647 encapsulation efficiency which is the focus of further particle technology investment than  
648 advanced pharmaceuticals.

649

## 650 REFERENCES

- 651 1. Smith BC, Wilson AH. Topical versus injectable analgesics in simple laceration repair: An  
652 integrative review. *JNP*. 2013;9(6):374-380.
- 653 2. Hogan ME, vanderVaart S, Permapaladas K, Márcio M, Einarson TR, Taddio A. Systematic  
654 review and meta-analysis of the effect of warming local anesthetics on injection pain. *Ann of*  
655 *Emerg Med*. 2011;58(1): 86-98.e1.
- 656 3. Capellan O, Hollander JE. Management of lacerations in the emergency department. *Emerg*  
657 *Med Clin North Am*. 2003;21(1):205-231.
- 658 4. Bekhit MH. The essence of analgesia and anagesics. Lidocaine for neural blockade.  
659 Cambridge University Press; 2011. p. 280-281.
- 660 5. Chale S, Singer AJ, Marchini S, McBride MJ, Kennedy D. Digital versus local anesthesia for  
661 finger lacerations: A randomized controlled trial. *Acad Emerg Med*. 2006;13(10):1046-1050.
- 662 6. Pregerson DB. Suturing and wound closure: How to achieve optimal healing. *Consultant*.  
663 2007;47(12):1-7.
- 664 7. Braga D, Chelazzi L, Greprioni F, Dichiaranta E, Chierotti MR, Gobetto R. Molecular salts of  
665 anaesthetic lidocaine with dicarboxylic acids: Solid-state properties and a combined  
666 structural and spectroscopic study. *Cryst Growth Des*. 2013;13:2564-2572.
- 667 8. Conroy PH, O'Rourke J. Tumescence anaesthesia. *The Surgeon* 2013;11:210-221.
- 668 9. Xia Y, Chen E, Tibbits DL, Reilley TE, McSweeney TD. Comparison of effect of lidocaine  
669 hydrochloride, buffered lidocaine, diphenhydramine, and normal saline after intradermal  
670 injection. *J Clin Anesth*. 2002;14:339-343.
- 671 10. Cepeda MS, Tzortzopoulou A, Thackrey M, Hudcova J, Gandhi PA, Schumann R. Adjusting  
672 the pH of lidocaine for reducing pain on injection. *Cochrane Database of Systematic*  
673 *Reviews* 12. 2010;DOI: 10.1002/14651858.
- 674 11. Columb MO, Ramsaran R. Local anaesthetic agents. *Anaesthe Intensive Care Med*. 2010;  
675 11(3):113-117.
- 676 12. Buhus G, Poap M, Desbrieres J. Hydrogels based on carboxymethylcellulose and gelatin for  
677 inclusion and release of chloramphenicol. *J Bioact Compat Pol*. 2009;24:525-545.
- 678 13. Mu C, Guo J, Li X, Lin W, Lin D. Preparation and properties of dialdehyde carboxymethyl  
679 cellulose crosslinked gelatin edible films. *Food Hydrocolloid*. 2012;27(1):22-29.
- 680 14. Becker DE, Reed KL. Local anaesthetics: Review of pharmacological consideration. *Anesth*  
681 *Prog*. 2012;59(2):90-102.
- 682 15. Alvarez-Lorenzo C, Blanco-Fernandez B, Puga AM, Concheiro A. Crosslinked ionic  
683 polysaccharides for stimuli-sensitive drug delivery. *Adv Drug Deliv Rev*. 2013;Article in press  
684 - <http://dx.doi.org/10.1016/j.addr.2013.04.016>
- 685 16. Hoare TR and Kohane DS. Hydrogels in drug delivery: progress and challenges (feature  
686 article). *Polym*. 2008;49(8):1993-2007.
- 687 17. Matricardi P, Meo CD, Coviello T, Hennink WE, Alhaique F. Interpenetrating polymer  
688 networks polysaccharide hydrogels for drug delivery and tissue engineering. *Adv Drug Deliv*  
689 *Rev* 2013; DOI: 10.1016.

- 690 18. Qiu Y, Park K. Environment-sensitive hydrogels for drug delivery. *Adv Drug Deliv Rev*  
691 2012;64(S):49-60
- 692 19. Patel SR, Lin ASP, Edelhauser HF, Prausnitz MR. Suprachoroidal drug delivery to the back  
693 of the eye using hollow microneedles. *Pharm Res* 2011;28(1):166-176.
- 694 20. Al-Qallaf B, Das DB. Optimization of square microneedle arrays for increasing drug  
695 permeability in skin. *Chem Eng Sci* 2008;63(9):2523-2535.
- 696 21. Henry S, McAllister DV, Allen MG, Prausnitz MR. Microfabricated microneedles: A novel  
697 approach to transdermal drug delivery. *J Pharm Sci.* 1998;87(8):922-925.
- 698 22. Donnelly RF, Singh TRR, Woolfson D. Microneedle-based drug delivery systems:  
699 Microfabrication, drug delivery, and safety. *Drug Deliv.* 2010;17(4):187–207.
- 700 23. Davis SP, Prausnitz MR, Allen MG. Fabrication and characterization of laser micromachined  
701 hollow microneedles. *Transducers.* 2003:1435-1438.
- 702 24. Zhang Y, Brown K, Siebenaler K, Determan A, Dohmeier D, Hansen K. Development of  
703 lidocaine-coated microneedle product for rapid, safe, and prolonged local analgesic action.  
704 *Pharm Res.* 2012;29(1):170–177
- 705 25. Ito Y, Ohta J, Imada K, Akamatsu S, Tsuchida N, Inoue G, Inoue N, Takada K. Dissolving  
706 microneedles to obtain rapid local anesthetic effect of lidocaine at skin tissue. *J Drug Target.*  
707 2013:1-6. DOI. 10.3109/1061186X.2013.811510.
- 708 26. Nayak A, Das DB. Potential of biodegradable microneedles as a transdermal delivery  
709 vehicle for lidocaine. *Biotechnol Lett.* 2013:DOI 10.1007/s10529-013-1217-3.
- 710 27. Küchler S, Strüver K, Wolfgang F. Reconstructed skin models as emerging tools for drug  
711 absorption studies. *Expert Opin Drug Met.* 2013: DOI 10.1517/17425255.2013.816284.
- 712 28. Karadzovska D, Brooks JD, Monteiro-Riviere NA, Riviere JE. Predicting skin permeability  
713 from complex vehicles. *Adv Drug Dev Rev.* 2013;65:265-277.
- 714 29. Van der Maaden K, Jiskoot W, Bouwstra J. Microneedle technologies for (trans)dermal drug  
715 and vaccine delivery. *J Control Release.* 2012;161(2):645-655.
- 716 30. Heilmann S, Küchler S, Wischke C, Lendlein A, Stein C, Schäfer-Korting M. A  
717 thermosensitive morphine-containing hydrogel for the treatment of large-scale skin wounds.  
718 *Int J Pharm.* 2013;444(1-2):96-102.
- 719 31. Han T, Das DB. Permeability enhancement for transdermal delivery of large molecule using  
720 low-frequency sonophoresis combined with microneedles. *J Pharm Sci.* 2013:1-9. DOI  
721 10.1002/jps.23662.
- 722 32. Auner BG, Valenta C. Influence of phloretin on the skin permeation of lidocaine from  
723 semisolid preparations. *Eur J Pharm Biopharm.* 2004;57(2):307-312.
- 724 33. Zhao X, Liu JP, Zhang X, Li Y. Enhancement of transdermal delivery of theophylline using  
725 microemulsion vehicle. *Int. J. Pharm.* 2006;327(1-2):58-64.
- 726 34. Kang L, Jun HW, McCall JW. Physicochemical studies of lidocaine menthol binary systems  
727 for enhanced membrane transport. *Int. J. Pharm.* 2000;206(1-2):35-42.
- 728 35. Poet TS, McDougal JN. Skin absorption and human risk assessment. *Chem-Biol Interact.*  
729 2002;140(1):19-34.
- 730 36. Naidu BVK, Paulson AT. A new method for the preparation of gelatin nanoparticles  
731 encapsulation and drug release characteristics. *J Appl Polym Sci.* 2011;121(6):3495-3500.

- 732 37. Al-Kahtani AA, Sherigara BS. Controlled release of theophylline through semi-  
733 interpenetrating network microspheres of chitosan-(dextran-g-acrylamide). *J Mater Sci:*  
734 *Mater Med.* 2009;20(7):1437-1445.
- 735 38. Marquez AL. Water in oil (w/o) and double (w/o/w) emulsions prepared with spans:  
736 microstructure, stability, and rheology. *Colloid Polym Sci.* 2007;285(10):1119-1128.
- 737 39. El-Mahrab-Robert M, Rosilio V, Bolzinger MA, Chaminade P, Grossiord JL. Assessment of  
738 oil polarity: Comparison of evaluation methods. *Int J Pharm.* 2008;348(1-2):89-94.
- 739 40. Chikh L, Delhorbe V, Fichet O. (Semi-) Interpenetrating polymer networks as fuel cell  
740 membranes. *J Membrane Sci.* 2011;368(1-2):1-17.
- 741 41. Jenkins AD, Kratochvíl P, Stepto RFT, Suter UW. Glossary of basic terms in polymer  
742 science. *Pure Appl Chem.* 1996;68(12):2304-2305.
- 743 42. Kajjari PB, Manjeshwar LS, Aminabhavi TM. Semi-interpenetrating polymer network  
744 hydrogel blend microspheres of gelatin and hydroxyethyl cellulose for controlled release of  
745 theophylline. *Ind Eng Chem Res.* 2011;50(13):7833-7840.
- 746 43. Rokhade AP, Agnihotri SA, Patil SA, Mallikarjuna NN, Kulkarni PV, Aminabhavi TM. Semi-  
747 interpenetrating polymer network microspheres of gelatin and sodium carboxymethyl  
748 cellulose for controlled release of ketorolac tromethamine. *Carbohydr Polym.* 2006;65(3):243-  
749 252.
- 750 44. Schramm LL. Emulsions, foams, and suspensions. 2005;Wiley-VCH:128-130
- 751 45. Riddick TM. Control of stability through zeta potential. 1968;Zeta Meter Inc. New York.
- 752 46. Koul V, Mohamed R, Kuckling D, Adler HJP, Choudhary V. Interpenetrating polymer network  
753 (IPN) nanogels based on gelatin and poly(acrylic acid) by inverse miniemulsion technique:  
754 Synthesis and characterization. *Colloid Surface B.* 2011;83(2):204-213.
- 755 47. Stenson RE, Constantino RT, Harrison DC. Interrelationships of hepatic blood flow, cardiac  
756 output, and blood levels of lidocaine in man. *Circulation.* 1971;43:205-211.
- 757 48. Greco FA. Therapeutic drug levels. MedlinePlus. A service of the U.S. National Library of  
758 Medicine; 2011. Available from: <http://www.nlm.nih.gov/medlineplus/ency/article/003430.htm>.  
759 [Website] Accessed: 22/04/13.
- 760 49. Todo H, Kimurae E, Yasuno H, Tokudome Y, Hashimoto F, Ikarashi Y, Sugibayashi K.  
761 Permeation pathway of macromolecules and nanospheres through skin. *Biol Pharm Bull.*  
762 2010;33(8):1394-1399.
- 763 50. Victoria Klang V, Schwarz JC, Haberfeld S, Xiao P, Wirth M and Valenta C. Skin integrity  
764 testing and monitoring of in vitro tape stripping by capacitance-based sensor imaging. *Skin*  
765 *Res Technol.* 2013;19:e259-e272

766

767  
768  
769

List of tables

Table i. Composition of chemical reagents used in formulating distinct LidH NaCMC/GEL hydrogel microparticles

Table i. Chemical reagents used for preparing different LidH NaCMC/GEL hydrogel microparticles

Drug Formulation	LidH (% w/w)	SPAN 80 (% w/w)	Paraffin oil (% w/w)	Deionised water (% w/w)	GEL (% w/w)	NaCMC (% w/w)	Acetic acid (~ % w/w)	Glutaraldehyde (% w/w)
LidH (2.4% w/w) NaCMC/GEL hydrogel microparticles	2.4	0.5	66.7	26.1	2.0	1.2	1.0	0.1
				25.6	2.5			
				25.3	2.8			
				24.9	3.2			
LidH NaCMC/GEL 1:1.6 mass ratio hydrogel microparticles	1.2	0.5	66.7	27.3	2.0	1.2	1.0	0.1
	2.4			26.1				
	2.8			25.8				
	7.0			21.5				
LidH NaCMC/GEL 1:2.3 mass ratio hydrogel microparticles	1.2	0.5	66.7	26.5	2.8	1.2	1.0	0.1
	2.4			25.3				
	2.8			25.1				
	7.0			20.7				
Unloaded NaCMC/GEL 1:2.3 mass ratio hydrogel microparticles	0	0.5	66.7	27.7	2.8	1.2	1.0	0.1

1

2

## List of figures

Fig. 1 a Crosslinking between sodium carboxymethyl cellulose (NaCMC) and gelatine A (GEL) via ether bonds between NaCMC and glutaraldehyde and schiff's base C=N linkage between glutaraldehyde and proline of GEL.  $R_1, R_2, R_3$  are repeating monomeric units of each polymer. b Ionic interactions between NaCMC, proline of GEL and LidH.  $R_1, R_2, R_3$  are repeating monomeric units of each polymer.

Fig. 2 Pathways for microneedle assisted and passive diffusion studies of LidH NaCMC/GEL on porcine skin via franz diffusion cells. Porcine skin was treated with microneedles before the addition of LidH NaCMC/GEL [A] for FDC. The direct addition [B] of LidH NaCMC/GEL is the start of the passive diffusion pathway. Sample LidH NaCMC/GEL [C] added to skin undergoes FDC experimentation for both microneedle and passive diffusion delivery. The FDC receptor amount was removed and centrifuged [D]. The supernatant removed was then analysed using HPLC-DA [E]. Inset is a stainless steel microneedle array with a length to width needle aspect ratio of 1:4 and a tip to tip needle spacing of 1100  $\mu\text{m}$ .

Fig. 3 Percentage encapsulation efficiency of LidH in hydrogel particles as a function of NaCMC:GEL mass ratio. The concentration of lidH in the initial emulsion was 2.4% w/w (Results represent arithmetic mean  $\pm$  SD values based on data from three reproduced hydrogel samples per mass ratio).

Fig. 4 a Dynamic viscosity of LidH NaCMC/GEL 1:2.3 hydrogels as a function of shear rate. b Dynamic viscosity of LidH 2.4% w/w in NaCMC/GEL hydrogels as a function of shear rate (Results represent data points from individual hydrogel samples per mass ratio).

Fig 5. Constant shear induction ( $200 \text{ s}^{-1}$ ) for lidocaine 2.4% w/w NaCMC/GEL hydrogel as a function of mass ratio of NaCMC to GEL (Results represent arithmetic mean  $\pm$  SD values based on data from two reproduced hydrogel samples per mass ratio).

Fig 6. LidH 2.4 % (w/w) NaCMC/GEL particle size distribution as a function of mass ratio of the two polymer (Results represent superimposed data points of each repeated hydrogel sample from a total of six individual hydrogel samples).

Fig. 7 a Zeta potential of LidH NaCMC/GEL 1:1.6 mass ratio microparticles. Values 1.2-7.0 are LidH loaded yields in % w/w. b Zeta potential of LidH (2.4-7.0% w/w) NaCMC/GEL mass ratio 1:1.6 and 1:2.3 microparticles. Values 2.4-7.0 are LidH loaded yields in % w/w. c Zeta potential of LidH (2.4% w/w) NaCMC/GEL mass ratio microparticles. d Zeta potential of LidH NaCMC/GEL mass ratio 1:2.3 microparticles. Values 2.4-7.0 are LidH loaded yields in % w/w (results represent arithmetic mean  $\pm$  SD values based on data from two reproduced hydrogel samples per mass ratio or concentration)

Fig. 8. pH effects on unencapsulated NaCMC/GEL 1:2.3 microparticles as a function of zeta potential. Experimental zeta (mV) ◆ Theoretical zeta (mV) ▲ (results represent arithmetic mean  $\pm$  SD values based on data from two hydrogel samples per mass ratio).

Fig. 9. Micrograph of LidH 2.4 % w/w NaCMC/GEL microparticles prepared using different polymeric ratios: a) 1:1.6 b) 1:2.0 c) 1:2.3 d) 1:2.7.

Fig. 10 a Cumulative amount of LidH permeated through skin from NaCMC/GEL within a four hour period. b Cumulative amount of LidH permeated through skin from NaCMC/GEL within a one hour period. c LidH (2.4 % w/w) NaCMC/GEL flux permeation through skin (results in (a) and (b) represent arithmetic mean  $\pm$  SD values based on data from two reproduced hydrogel samples per mass ratio. Result in (c) represents random error of two reproduced mass ratio samples for passive diffusion and microneedle values based on 90 % confidence level).



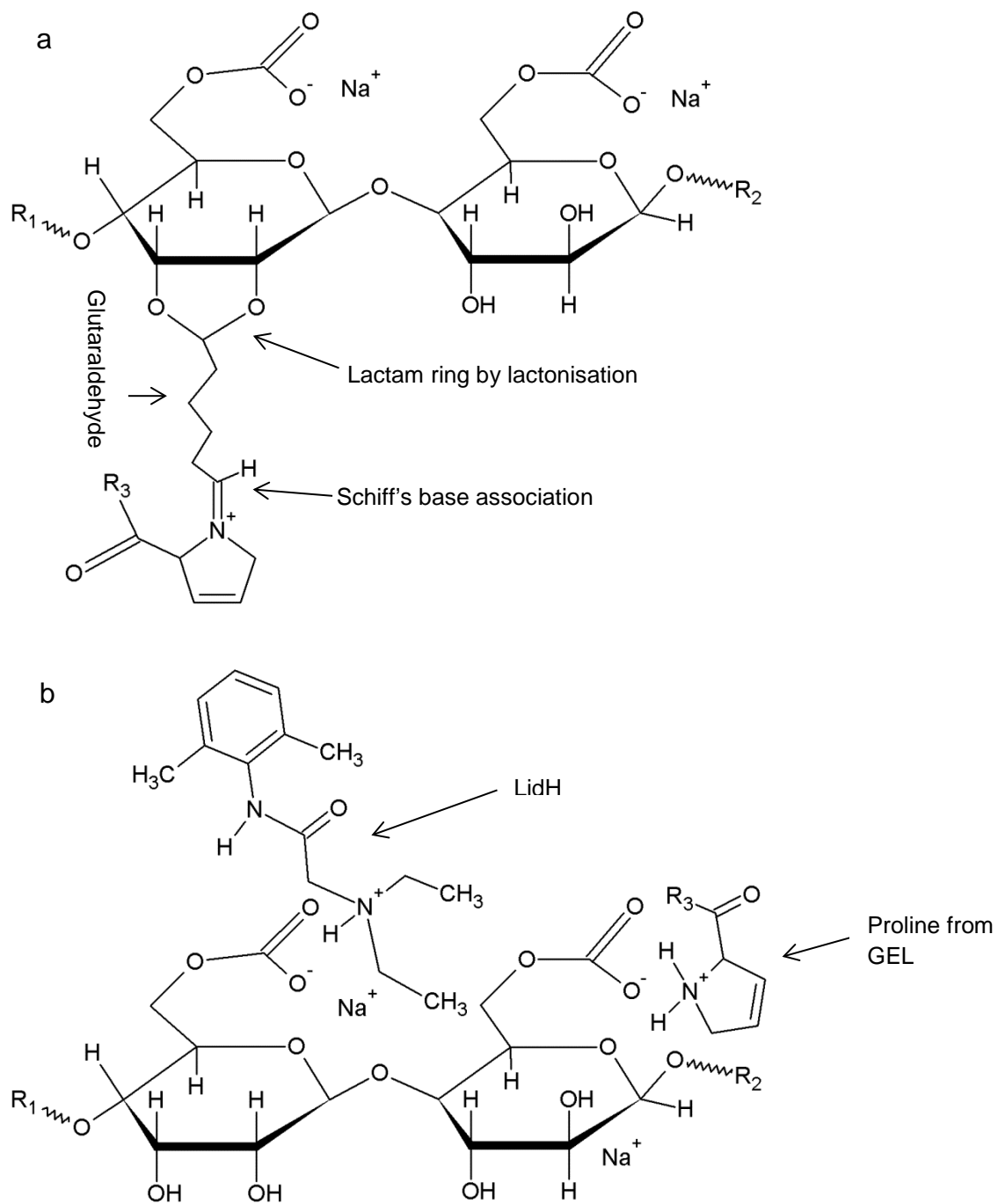


Fig. 1 a Crosslinking between sodium carboxymethyl cellulose (NaCMC) and gelatine A (GEL) via ether bonds between NaCMC and glutaraldehyde and schiff's base C=N linkage between glutaraldehyde and proline of GEL.  $R_1$ ,  $R_2$ ,  $R_3$  are repeating monomeric units of each polymer. b Ionic interactions between NaCMC, proline of GEL and LidH.  $R_1$ ,  $R_2$ ,  $R_3$  are repeating monomeric units of each polymer.

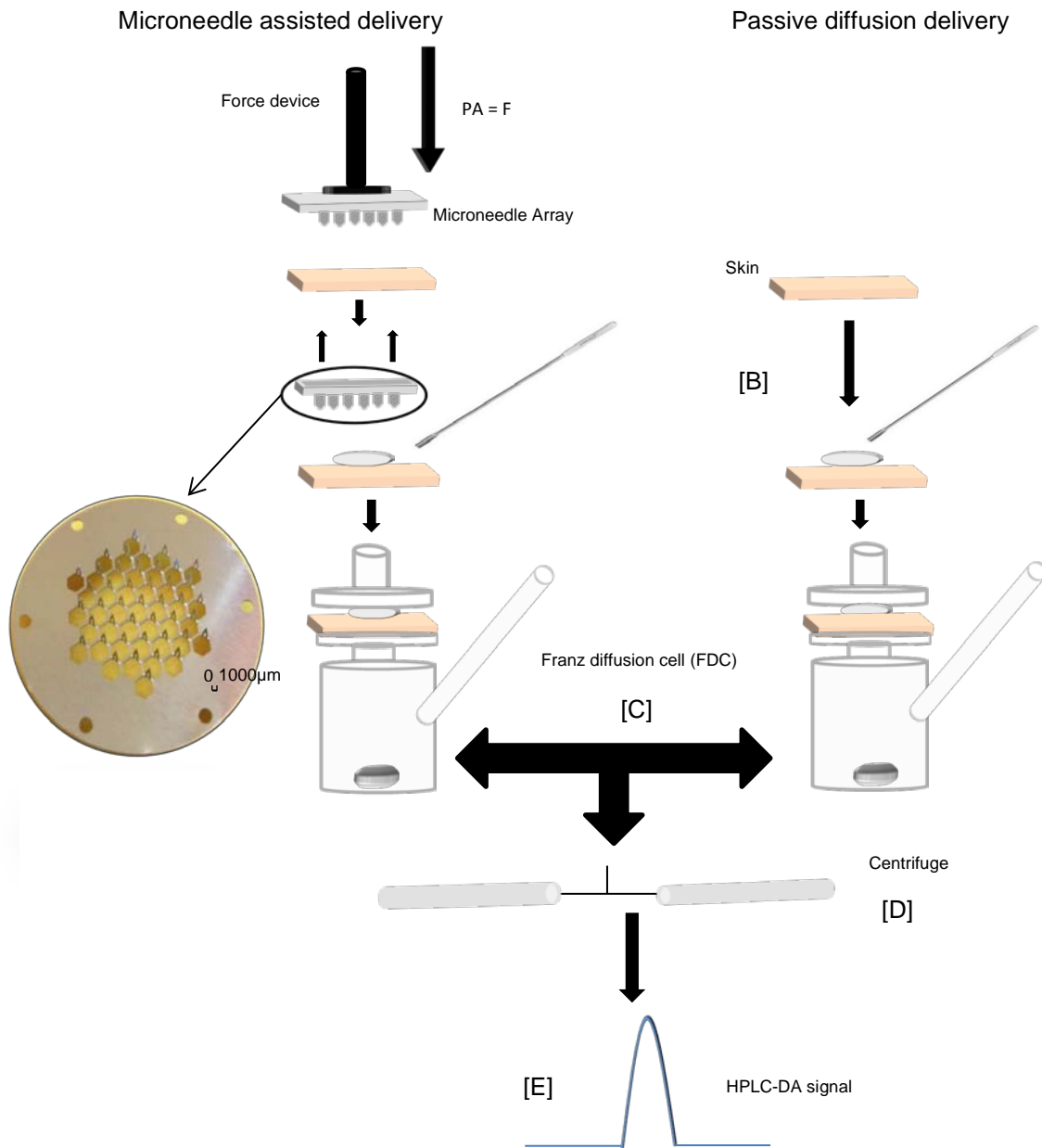


Fig. 2 Pathways for microneedle assisted and passive diffusion studies of LidH NaCMC/GEL on porcine skin via franz diffusion cells. Porcine skin was treated with microneedles before the addition of LidH NaCMC/GEL [A] for FDC. The direct addition [B] of LidH NaCMC/GEL is the start of the passive diffusion pathway. Sample LidH NaCMC/GEL [C] added to skin undergoes FDC experimentation for both microneedle and passive diffusion delivery. The FDC receptor amount was removed and centrifuged [D]. The supernatant removed was then analysed using HPLC-DA [E]. Inset is a stainless steel microneedle array with a length to width needle aspect ratio of 1:4 and a tip to tip needle spacing of 1100  $\mu\text{m}$ .

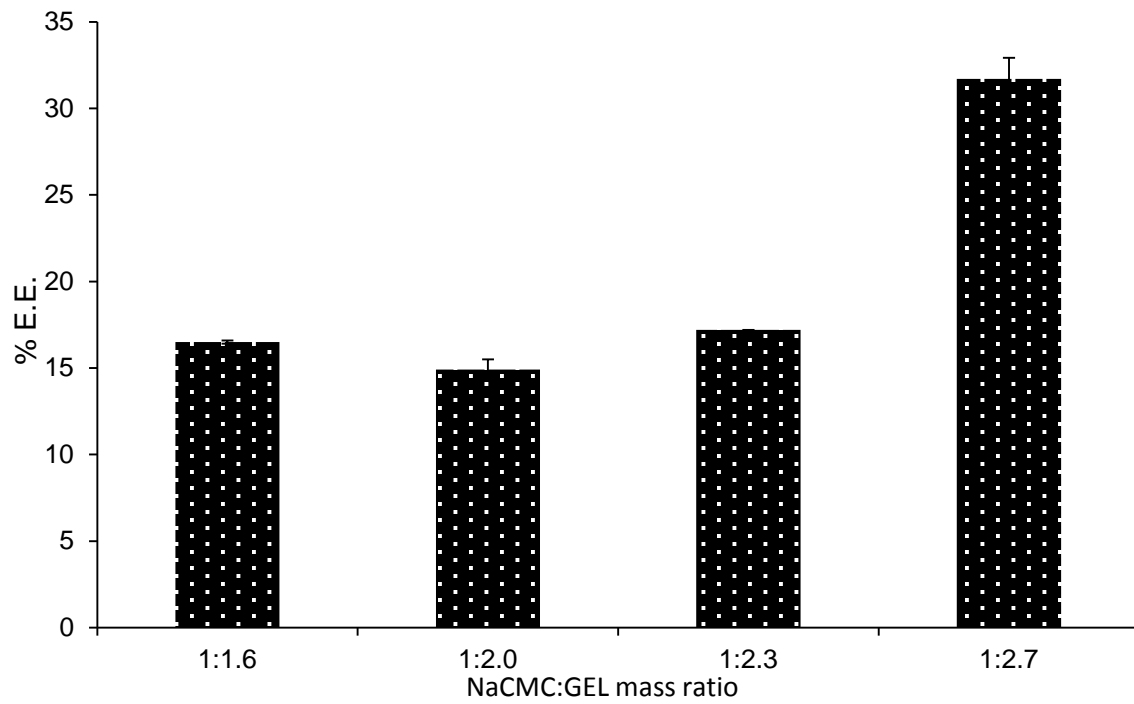


Fig. 3 Percentage encapsulation efficiency of LidH in hydrogel particles as a function of NaCMC:GEL mass ratio. The concentration of lidH in the initial emulsion was 2.4% w/w (Results represent arithmetic mean  $\pm$  SD values based on data from three reproduced hydrogel samples per mass ratio).

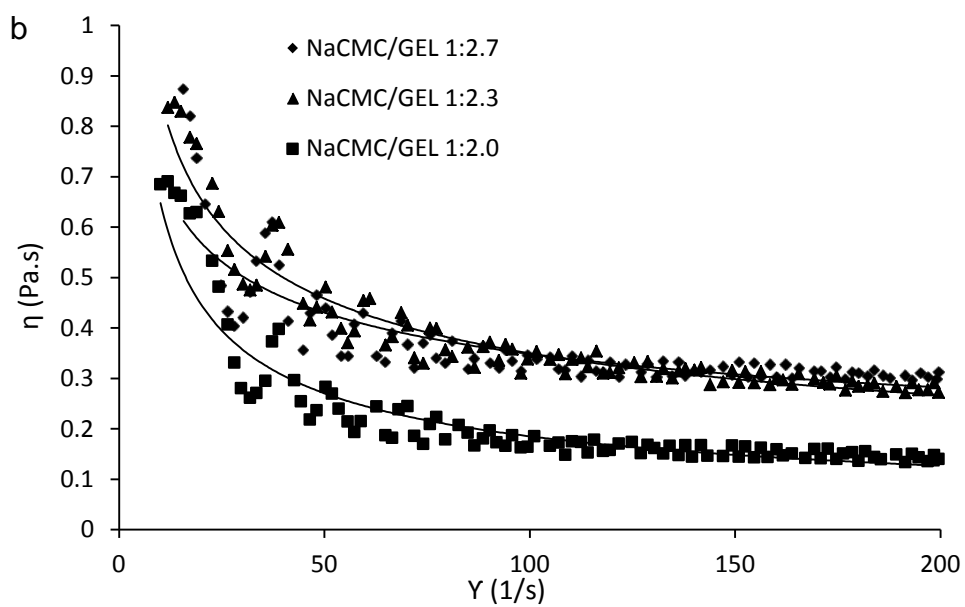
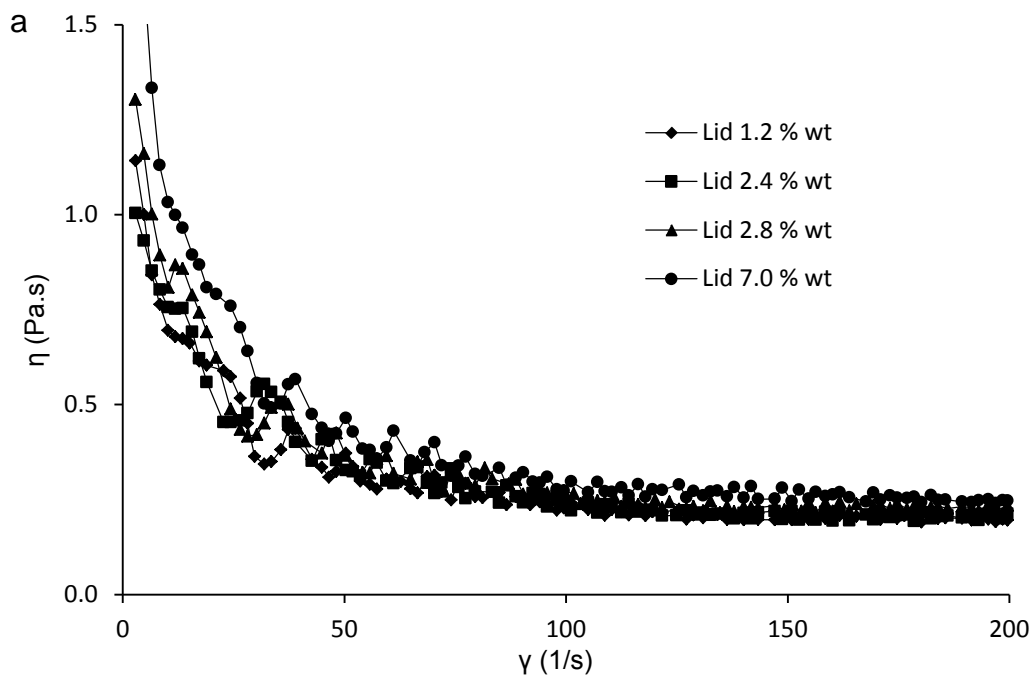


Fig. 4 a Dynamic viscosity of LidH NaCMC/GEL 1:2.3 hydrogels as a function of shear rate. b Dynamic viscosity of LidH 2.4% w/w in NaCMC/GEL hydrogels as a function of shear rate (Results represent data points from individual hydrogel samples per mass ratio).

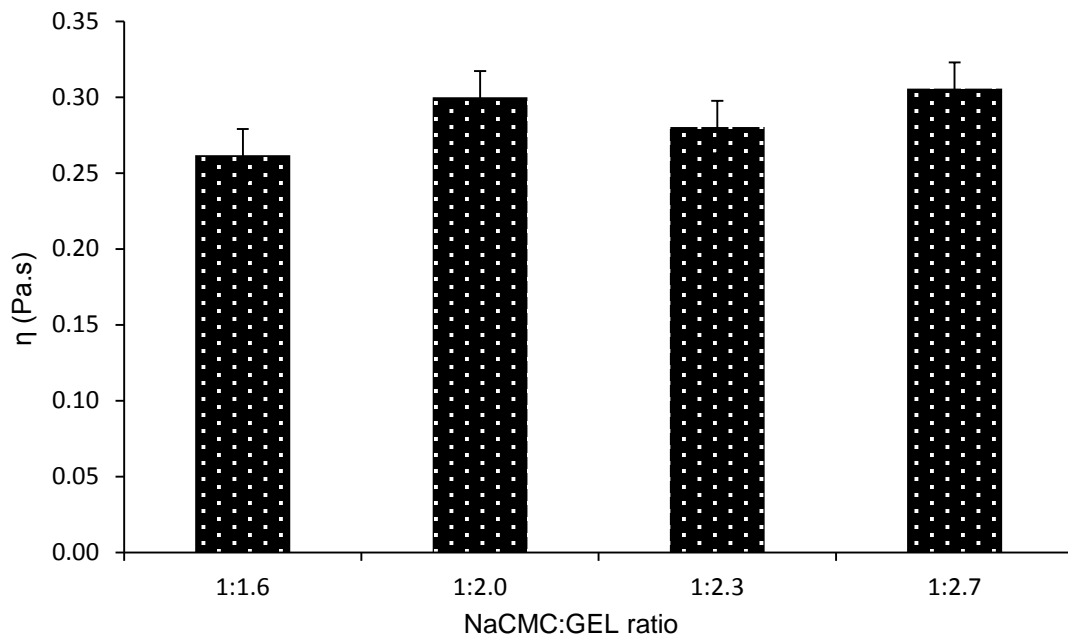


Fig. 5 Constant shear induction ( $200 \text{ s}^{-1}$ ) for lidocaine 2.4% w/w NaCMC/GEL hydrogel as a function of mass ratio of NaCMC to GEL (Results represent arithmetic mean  $\pm$  SD values based on data from two reproduced hydrogel samples per mass ratio).

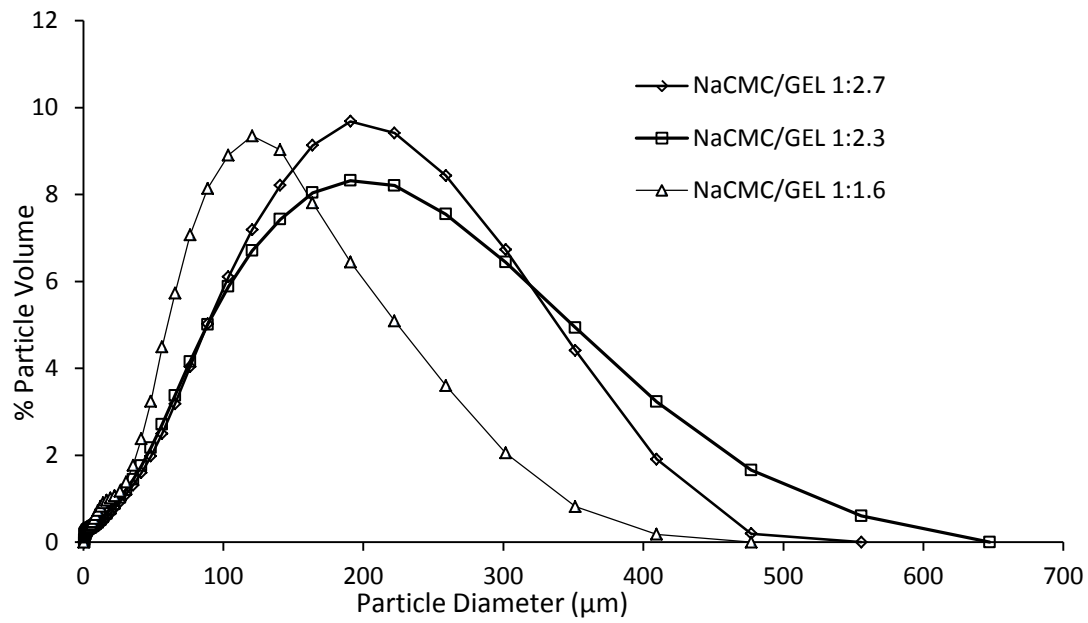


Fig. 6 LidH 2.4 % (w/w) NaCMC/GEL particle size distribution as a function of mass ratio of the two polymer (Results represent superimposed data points of each repeated hydrogel sample from a total of six individual hydrogel samples).

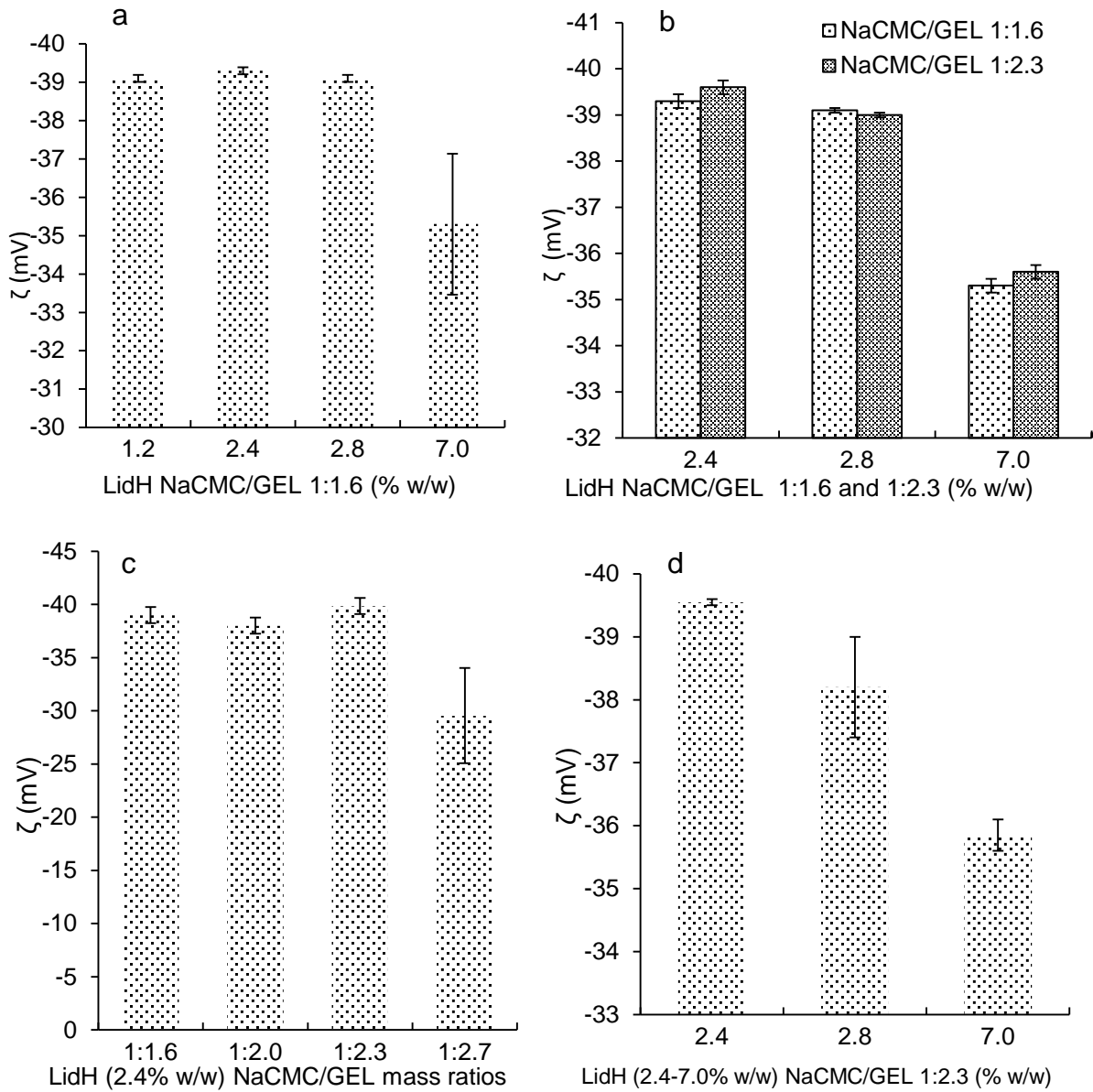


Fig. 7 a Zeta potential of LidH NaCMC/GEL 1:1.6 mass ratio microparticles. Values 1.2-7.0 are LidH loaded yields in % w/w. b Zeta potential of LidH (2.4-7.0% w/w) NaCMC/GEL mass ratio 1:1.6 and 1:2.3 microparticles. Values 2.4-7.0 are LidH loaded yields in % w/w. c Zeta potential of LidH (2.4% w/w) NaCMC/GEL mass ratio microparticles. d Zeta potential of LidH NaCMC/GEL mass ratio 1:2.3 microparticles. Values 2.4-7.0 are LidH loaded yields in % w/w (results represent arithmetic mean  $\pm$  SD values based on data from two reproduced hydrogel samples per mass ratio or concentration)

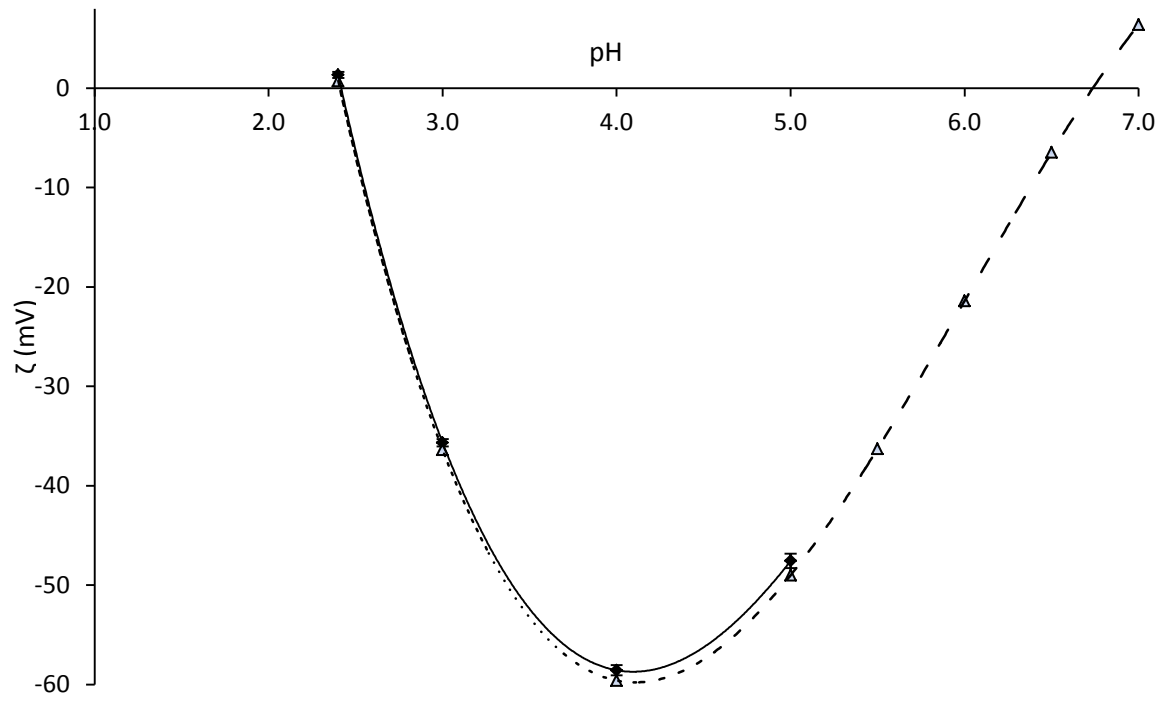


Fig 8 pH effects on unencapsulated NaCMC/GEL 1:2.3 microparticles as a function of zeta potential. Experimental zeta (mV) ◆ Theoretical zeta (mV) ▲ (results represent arithmetic mean  $\pm$  SD values based on data from two hydrogel samples per mass ratio).



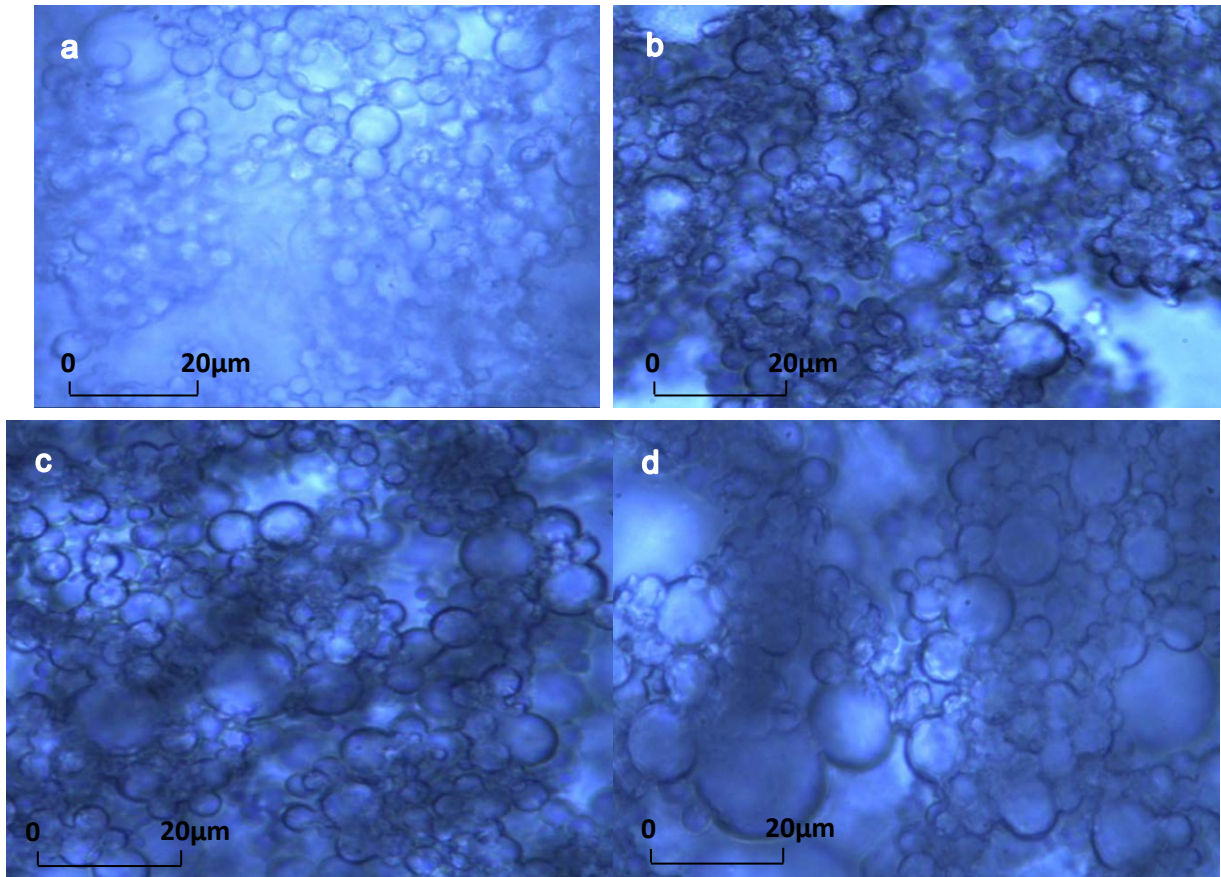


Fig. 9 Micrograph of LidH 2.4 % w/w NaCMC/GEL microparticles prepared using different polymeric ratios: a) 1:1.6 b) 1:2.0 c) 1:2.3 d) 1:2.7.

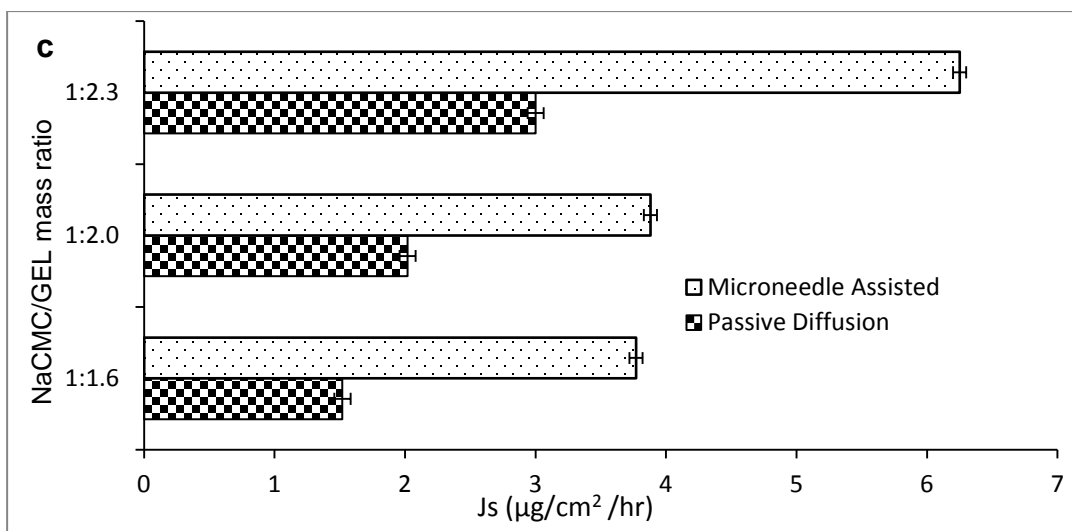
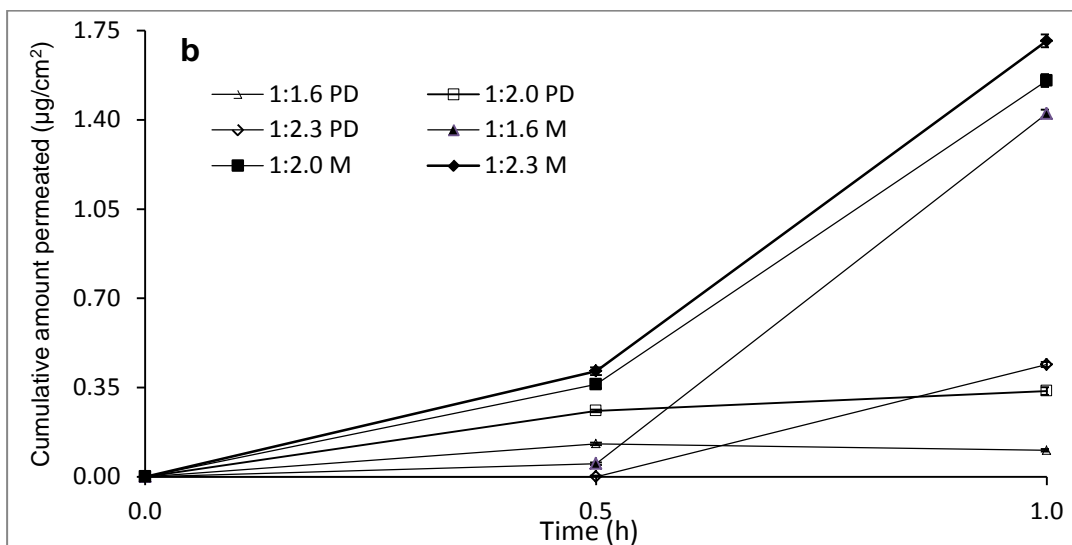
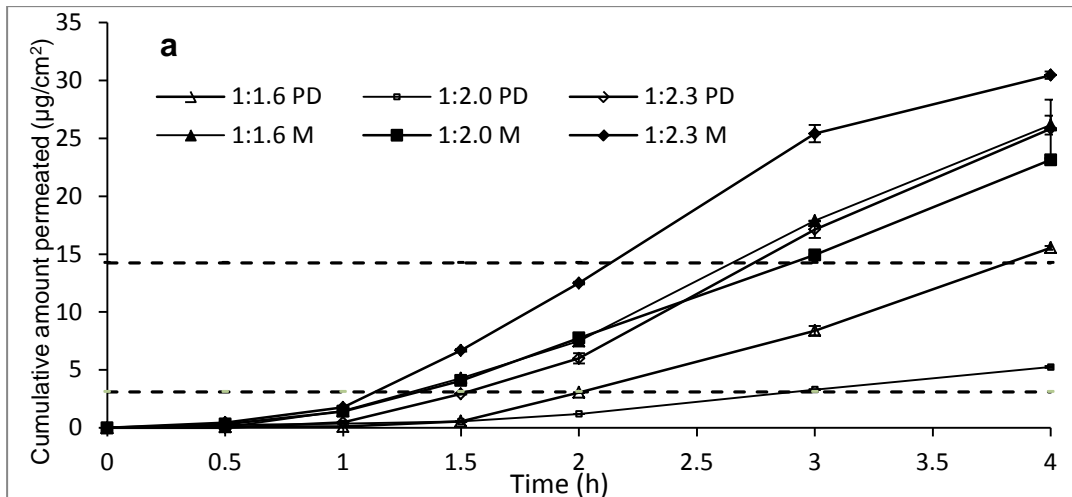


Fig. 10 a Cumulative amount of LidH permeated through skin from NaCMC/GEL within a four hour period. b Cumulative amount of LidH permeated through skin from NaCMC/GEL within a one hour period. c LidH (2.4 % w/w) NaCMC/GEL flux permeation through skin (results in (a) and (b) represent arithmetic mean  $\pm$  SD values based on data from two reproduced hydrogel samples per mass ratio. Result in (c) represents random error of two reproduced mass ratio samples for passive diffusion and microneedle values based on 90 % confidence level).